SEDIMENT CONTROL IN BRIDGE WATERWAYS

by

A. Jacob Odgaard and Yalin Wang

Sponsored by the
Highway Division of the Iowa Department of Transportation
and
the Iowa Highway Research Board
Project HR-307

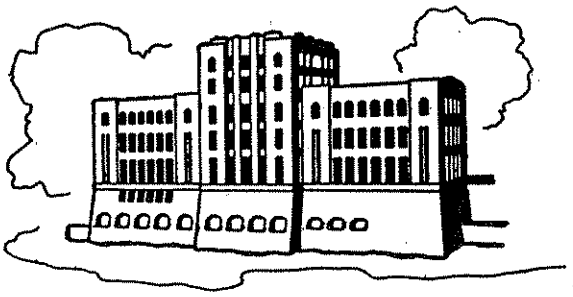

IIHR Report No. 336

Iowa Institute of Hydraulic Research
The University of Iowa
Iowa City, Iowa 52242-1585

February 1990

SEDIMENT CONTROL IN BRIDGE WATERWAYS

by

A. Jacob Odgaard and Yalin Wang

Sponsored by the

Highway Division of the Iowa Department of Transportation
and
the Iowa Highway Research Board
Project HR-307

IIHR Report No. 336

Iowa Institute of Hydraulic Research
The University of Iowa
Iowa City, Iowa 52242-1585

February 1990

Acknowledgements

The Iowa Highway Research Board participated in this study. Funding was provided by the Highway Division of the Iowa Department of Transportation and the National Science Foundation.

A number of individuals provided input and help during the study. Among them are: Vernon Marks, Materials Research, and Mark Looschen, Bridge Design, Iowa DOT, Ames, Iowa; Robert L. Haylock, Butler County Engineer, Allison, Iowa; and James R. Goss, Supervisor, IIHR, and his staff. The success of the study is to a great extent due to these individuals.

The study is in part the basis for the second author's Ph.D. dissertation.

The opinions, findings and conclusions expressed in this report are those of the authors and not necessarily those of the Highway Division of the Iowa Department of Transportation.

ABSTRACT

The objective of this study was to develop guidelines for use of the Iowa Vanes technique for sediment control in bridge waterways. Iowa Vanes are small flow-training structures (foils) designed to modify the near-bed flow pattern and redistribute flow and sediment transport within the channel cross section. The structures are installed at an angle of attack of 15 - 25° with the flow, and their initial height is 0.2 - 0.5 times water depth at design stage. The vanes function by generating secondary circulation in the flow. The circulation alters magnitude and direction of the bed shear stress and causes a reduction in velocity and sediment transport in the vane controlled area. As a result, the river bed aggrades in the vane controlled area and degrades outside.

This report summarizes the basic theory, describes results of laboratory and field tests, and presents the resulting design procedure.

Design graphs have been developed based on the theory. The graphs are entered with basic flow variables and desired bed topography. The output is vane layout and design. The procedure is illustrated with two numerical examples prepared with data that are typical for many rivers in Iowa and the midwest. The report also discusses vane material.

In most applications, the vane height will be between 30% and 50% of bankfull flow depth and the vane length will be two to three times vane height. The vanes will be placed in arrays along the bank of the river. Each array will contain two or more vanes. The vanes in an array will be spaced laterally a distance of two to three times vane height. The streamwise spacing between the arrays will be 15 to 30 times vane height, and the vane-to-bank distance will be three to four times vane height. The study also show that the first (most upstream) array in the vane system must be located a distance of at least three array spacings upstream from the bridge, and there must be at least three arrays in the system for it to be effective at and downstream from the third array.

TABLE OF CONTENTS

LIST OF SYMBOLS

The following symbols are used in this report:

A = area of vane field;
A_v = reciprocal vane density;
B = function (Eq. 23);
b = channel width;
c_D = drag coefficient (Eqs. 9 and 13);
c_L = lift coefficient (Eqs. 8 and 12);
D = sediment grain size;
d = flow depth;
F = stress terms in Eqs. 16-18;
F_D = drag force (Eq. 9), and particle densimetric Froude number (Eq. 34);
F_L = lift force (Eq. 8);
f = Darcy-Weisbach's friction factor;
f_v = function (Eq. 6);
G = function (Eq. 33);
g = acceleration due to gravity;
H = exposed vane height;
H_o = initial (design) vane height;
L = vane length;
m = friction parameter ($= \kappa\sqrt{8/f}$);
N = number of vanes;
n = cross-stream coordinate (Fig. 1);
q = bedload transport rate;
r = local radius of curvature;
S, S_r = streamwise and transverse slope of water surface;
s = downstream coordinate (Fig. 1);
u,v,w = time-averaged velocity components in s-, n-, and z-directions, respectively;
$\bar{u}$, $\bar{v}$ = depth-averaged values of u and v;
z = vertical coordinate (Fig. 1);
α = vane angle of attack with flow;
Δ = specific weight of submerged sediment [$= (\rho_s - \rho)/\rho$];
δ_b = distance from bank to vane;

δ_s,δ_n = vane spacing in streamwise and transverse direction, respectively;
θ = Shields' parameter;
κ = von Karman's constant;
λ = vane interaction coefficient;
ν = kinematic viscosity;
ρ = fluid density;
ρ_s = sediment density;
τ = shear stress; and
ε = eddy viscosity.

Subscripts

b = near-bed;
n = transverse component;
o = initial, cross-sectional average, pre-vane parameter;
s = streamwise component, surface value; and
v = vane

LIST OF FIGURES

SEDIMENT CONTROL IN BRIDGE WATERWAYS

I. INTRODUCTION

Bridge waterways are prone to sediment problems. Bars of sand tend to form immediately upstream or downstream from or at bridges causing the flow to pass the bridge in an undesirable manner. The flood conveyance capacity is reduced when such bars form. As a result, flood damages increase, and abutments, piers and river banks become subject to erosion. The problems arise because of the unsteady and often unpredictable behavior of the waterways. Although bridges are constructed to permit free passage of the flow in the waterways, there are numerous examples of how even minor man made interferences with the flow, such as a bridge pier, can trigger major alterations in river alignment and depositional patterns of the sediment. Evidence of the problem is seen at crossings of virtually all of the major rivers in Iowa. Common manifestations of the problems are complaints (and suits) from landowners, who are experiencing an increase in soil loss and flood damages due to more frequent overbank flows.

The sedimentation problem in bridge waterways are in general due to a combination of inter-related factors, the most important of which are (1) meander migration, (2) channelization, and (3) backwater on the flood plain created by the road embankments. The conditions are generally complex, and there are few standard procedures available for predicting the resulting sedimentation pattern in the main channel. In view of the large investments that are usually involved in river training and control, the attitude among highway engineers has often been one of "wait-and-see". Action is generally taken only when the cost of providing the necessary training structures is less than that associated with traffic delays and repairing of damages.

A simple solution to the problem is indicated following the recent development of the Iowa Vane technique (Iowa Highway Research Board Projects HR-255 and HR-274). Iowa vanes are small flow-training structures (foils) designed to modify the near-bed flow pattern and redistribute flow and sediment transport within the channel cross section. The structures are installed at an angle of attack of 15-25° with the flow, and their initial height is 0.2-0.5 times water depth at design stage. The vanes function by generating secondary circulation in the flow. The circulation alters magnitude and direction of the bed shear stress and causes a reduction in velocity and sediment transport in the vane controlled area. As a result, the river bed aggrades in the vane controlled area and degrades outside.

The technique was originally developed to stop or reduce bank erosion in river curves. In this application the vanes are laid out so that the vane generated secondary cur-

rent eliminates the centrifugally induced secondary current, which is the root cause of bank undermining. The centrifugally induced secondary current in river bends is the result of the interaction between the vertical gradient of velocity and the curvature of flow. It causes high-velocity surface current to be moved outward and low-velocity near-bed current inward. The increase in velocity at the outer bank causes flow depth to increase and the bank to steepen and become unstable. By directing the near-bed current toward the outer bank, the submerged vanes counter the centrifugally induced secondary current and, thereby, inhibit bank erosion. The vanes can be laid out to make the water and sediment move through a river curve as if it were straight. The first field test with this application was in a bend of East Nishnabotna River, Iowa (Odgaard and Mosconi 1987). The results of this test are very satisfactory. Other successful field tests are reported by Fukuoka and Watanabe (1989) and Kunzig (1989).

The technique was subsequently developed to ameliorate shoaling problems in rivers. This application was suggested by laboratory tests (Odgaard and Spoljaric 1986) in which vanes were laid out to change the cross-sectional profile of the bed in a straight channel. It was found that significant changes in depth can be achieved without causing significant changes in cross-sectional area, energy slope and downstream sediment transport. This is because the vane induced secondary current changes the direction of the bed shear stress by only a small amount. It was this observation that suggested that vanes can be used to control the depositional patterns of sediment in bridge waterways. Prototype experience with vanes in straight channels has been obtained from two installations, one at Iowa Resources power plant on the Missouri River near Council Bluffs, the other at a highway crossing of West Fork Cedar River, Butler County, Iowa.

These field experiences, and further experimental and theoretical studies have resulted in an improved understanding of the functioning of vanes and an improved design basis. This report summarizes the most significant improvements. Following a brief description of the theory, the report describes results of the laboratory experiments conducted to verify the theory. Field data taken at the Butler County installation are subsequently analyzed and compared with the theory. The report concludes by summarizing the resulting design procedures.

Readers who are mostly interested in the application of the technique may proceed to Section 4 of Chapter II (page 15). The material discussed in Section 4 and subsequent Chapters is self-contained and does not require a complete understanding of the theoretical background.

II. THEORY

The theory develops the relationship between vane characteristics and induced bed shear stresses. This relationship is then incorporated into the governing flow equations, which are solved to obtain flow and depth distributions within and outside the vane controlled area.

1. Vane Induced Bed Shear Stresses

A submerged vane at a small angle of attack with the flow, α, induces a horizontal circulation in the flow downstream (Figure 1). The circulation arises because the pressure difference between the two sides of the vane causes flow from the high pressure side to flow over the top of the vane and down on the low pressure side. The resulting vortex (tip vortex) is carried with the flow downstream where it gives rise to a secondary or helical motion of the flow and associated changes in bed shear stress and bed topography (Figure 2). These changes can be calculated.

The profile of the mean velocity is represented by a power law

$$u = \frac{m+1}{m} \left(\frac{z}{d}\right)^{1/m} \bar{u} \tag{1}$$

in which u = point velocity at height z above the bed, d = flow depth, $\bar{u}$ = depth-averaged velocity, and m = resistance coefficient which is related to Darcy-Weisbach's friction factor f as $m = \kappa \sqrt{8/f}$ (Zimmermann and Kennedy 1978); κ = von Karman's constant ($\simeq$ 0.4). Hence, $m = \kappa \bar{u}/\sqrt{gSd}$, where S = longitudinal slope of the water surface, and g = acceleration due to gravity.

The tip vortex is described as a steady potential vortex, i.e., a vortex maintained by angular momentum provided by the core. Its strength decays due to viscosity as the vortex is transported downstream. Consequently, the tangential velocity perpendicular to the core axis is

$$v = \sum_{j=1}^{\infty} \frac{\Gamma}{2\pi r_j} \left[1 - \exp\left(-\frac{u}{4\varepsilon x} r_j^2\right)\right] \tag{2}$$

in which r_j = distance from the core of vortex j, ε = eddy viscosity, x = downstream distance, and Γ = horizontal circulation at x = 0. The summation includes contributions from

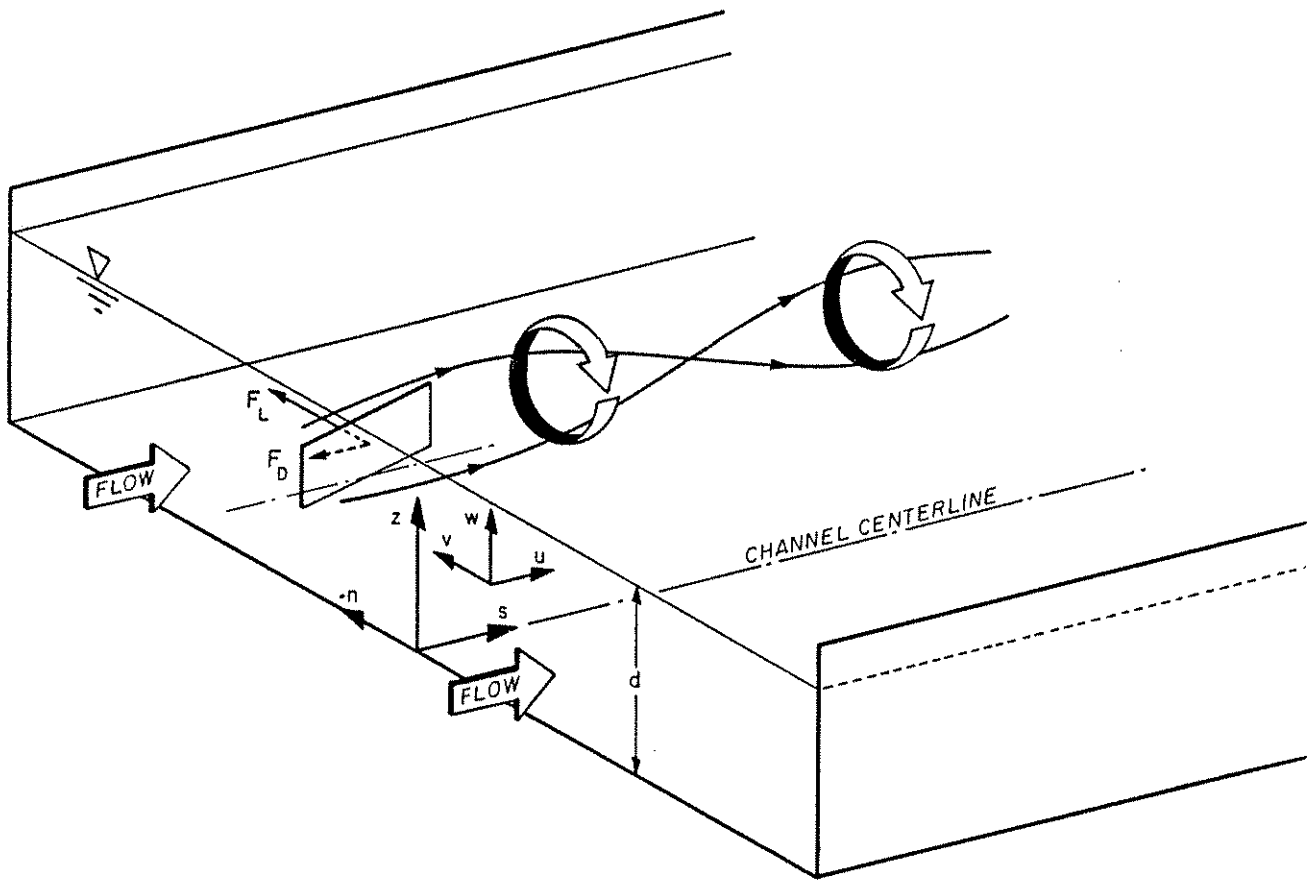

Figure 1. Schematic of flow situation showing vane induced circulation.

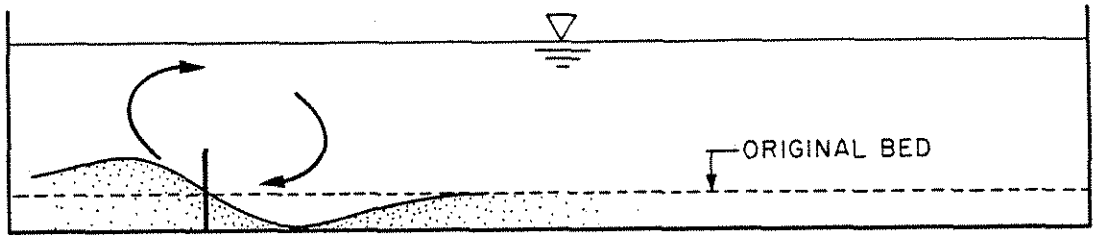

Figure 2. Schematic showing vane induced change in bed profile.

the images of the tip vortex with respect to the water surface and streambed. Because of the pressure difference between the vane's pressure and suction sides, the vortex core is located somewhat below the top elevation of the vane. Calculations (Milne-Thomson 1966 p. 209) and data (Odgaard and Spoljaric 1989, and Wang 1990) show that the core is about 0.2 times the vane height below the top elevation of the vane. The downstream decay of the vortex is the result of turbulence generated by both bed resistance and vane induced shear flow. Bed resistance is the major factor, and the decay can be evaluated relatively accurately by assuming that the profile of ε is parabolic (Odgaard and Spoljaric 1989). In this case $\varepsilon/u \propto \kappa^2 d/(6m)$. The horizontal circulation Γ can be evaluated by relating it to the horizontal lift force, F_L, that the flow exerts on the vane (Figure 1). According to the Kutta-Joukowskii theorem (Sabersky and Acosta 1964) this force is proportional to the vertical circulation around the vane associated with the "shift" of the rear stagnation point to the trailing edge of the vane, which in turn, is equal to the horizontal circulation Γ (Helmholz's second theorem). The relation reads $F_L = \rho\Gamma uH$, where ρ = fluid density and H = vane height.

From the velocity field thus calculated the near-bed transverse velocity component is obtained by projection,

$$v_{vn} = \frac{F_L}{2\pi\rho uH} \sum_{j=1}^{\infty} \frac{1}{r_j}\left[1-\exp\left(-\frac{3}{2}\frac{m}{\kappa^2 x_d} r_j^2\right)\right]\frac{z_j}{r_j} \tag{3}$$

in which z_j = vertical distance from channel bed to vortex core, and subscript n denotes the transverse direction. The induced transverse bed shear stress, τ_{vn}, can now also be calculated. It is reasonable to expect that the angle that the bed shear stress is deflected as a result of the induced circulation is the same as that of the velocity so that

$$\frac{\tau_{vn}}{\tau_{bs}} = \frac{v_{vn}}{u_b} \tag{4}$$

where τ_{bs} = streamwise bed shear stress = $\rho\kappa^2\bar{u}^2/m$, and u_b = near-bed value of u. The value of u_b is a certain fraction of $\bar{u}$, i.e., $\bar{u} = ku_b$, where k = function of m. By substituting Eq. 3 into Eq. 4, the transverse bed shear stress is

$$\tau_{vn} = F_L f_v \tag{5}$$

where
$$f_v = \frac{k^2\kappa^2}{2\pi mH} \sum_{j=1}^{\infty} \frac{1}{r_j}\left[1\text{-}\exp\left(-\frac{3}{2}\frac{m}{\kappa^2 xd} r_j^2\right)\right]\frac{z_j}{r_j} \tag{6}$$

It follows that the streamwise (s) component of the induced bed shear stress is

$$\tau_{vs} = F_D f_v \tag{7}$$

where F_D = drag force associated with F_L.

Both F_L and F_D are most easily calculated by relating them to dynamic pressure as

$$F_L = \frac{1}{2} c_L \rho L \int_o^H u^2 dz \tag{8}$$

and
$$F_D = \frac{1}{2} c_D \rho L \int_o^H u^2 dz \tag{9}$$

in which L = vane length, and c_L, c_D = lift and drag coefficients. By substituting Eq. 1 into Eqs. 8 and 9, the lift and drag forces are

$$F_L = \frac{1}{2} \rho c_L HL \bar{u}^2 \frac{(m+1)^2}{m(m+2)} \left(\frac{H}{d}\right)^{2/m} \tag{10}$$

and
$$F_D = \frac{c_D}{c_L} F_L \tag{11}$$

By assuming that the distribution of the vertical circulation around the vane is elliptic being maximum at the bed and zero at the top of the vane, the lift coefficient is (Odgaard and Mosconi 1987)

$$c_L = \frac{2\pi\alpha}{1 + \frac{L}{H}} \tag{12}$$

The corresponding drag coefficient is determined by

$$c_D = \frac{1}{2\pi} \frac{L}{H} c_L^2 \tag{13}$$

The flow area affected by a single vane is limited. In the transverse direction the vane has little impact beyond about three times vane height. A wider area is affected if two or more vanes are employed. If the vanes are arranged in an array as shown in Figures 3 and 4, the width of the affected area is increased. However, because of interaction between tip vortices, the strength of the induced circulation is then less than that obtained by simple superposition of individual vorticity fields. The interaction between two or more tip vortices, and its effect on total induced circulation, is described by an interaction model similar to that used for biplanes. According to this model, which is described in detail by Wang (1989), the total circulation induced by an array of equally sized equally angled vanes is obtained by adding the circulations of individual vanes provided that these are adjusted by an interaction coefficient λ, which is a function of vane spacing δ_n and vane dimensions H and L. It follows from this model that in order for a vane array to generate a coherent circulation downstream, vane spacing must be less than about two to three times vane height. When the spacing is two-to-three times vane height, λ is of the order of 0.9. If the spacing is larger, the vane array will generate a system of individual vortices and be less efficient. The coefficient λ is incorporated in the function f_v so that the resulting stress distribution downstream from a vane array is obtained by summation of the stress distributions associated with the individual vanes in the array.

In order to sustain a certain induced circulation and induced bed shear stress downstream, the vane array must be repeated at intervals in the downstream direction. The distance between the arrays, δ_s, depends on the design objective, which must stipulate lower limits on induced stresses. If, for example, the vanes are to eliminate the transverse bed shear stresses associated with the secondary current in river curves, τ_{bn}, then δ_s must be selected such that induced transverse bed shear stress is everywhere greater than - τ_{bn}. Within a vane field consisting of equal-sized, equal-spaced vanes, the area averaged induced bed shear stresses are

$$\bar{\tau}_{vn} = \frac{F_L \lambda}{A_v} \tag{14}$$

and

$$\bar{\tau}_{vs} = \frac{F_D \lambda}{A_v} \tag{15}$$

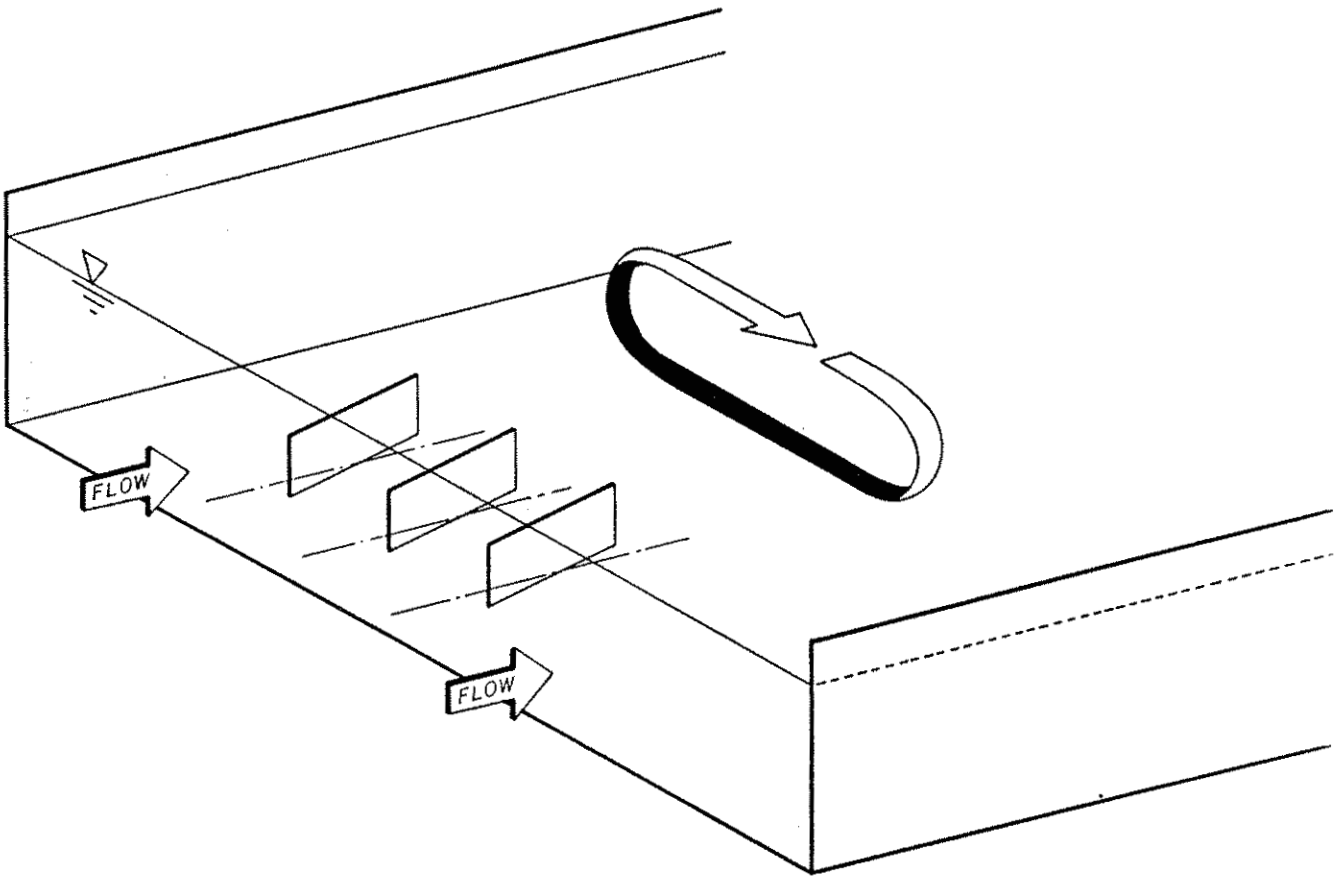

Figure 3. Schematic showing circulation induced by array of three vanes.

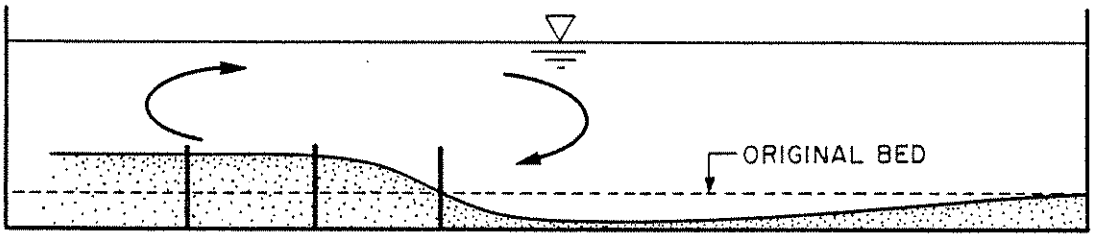

Figure 4. Schematic showing change in bed profile induced by array of three vanes.

in which $A_v = \delta_n \delta_s$, and overbars indicate area averaging. It follows that if the vane field covers an area A and the total number of vanes is N, then $A_v = A/N$.

In the subsequent analysis it is assumed that the vanes affect the flow field through these induced bed shear stresses.

2. Governing Equations

The coordinate system used is shown in Figure 1. The s-axis is along the channel centerline, positive in the streamwise direction; the n-axis is perpendicular to the s-axis and positive toward the concave bank; and the z-axis is vertically upward from the streambed. If the channel is straight, the n-axis is positive toward the bank that is concave in the preceding bend upstream. The velocity components (time averaged) in the s, n, and z directions are denoted u, v, and w, respectively. The equations of motion are (Rozovskii 1957)

$$u\frac{\partial u}{\partial s} + v\frac{\partial u}{\partial n} + w\frac{\partial u}{\partial z} + \frac{uv}{r} = -\frac{1}{\rho}\frac{\partial p}{\partial s} + F_s \tag{16}$$

$$u\frac{\partial v}{\partial s} + v\frac{\partial v}{\partial n} + w\frac{\partial v}{\partial z} + \frac{u^2}{r} = -\frac{1}{\rho}\frac{\partial p}{\partial n} + F_n \tag{17}$$

$$u\frac{\partial w}{\partial s} + v\frac{\partial w}{\partial n} + w\frac{\partial w}{\partial z} + g = -\frac{1}{\rho}\frac{\partial p}{\partial z} + F_z \tag{18}$$

in which r = local radius of curvature; p = pressure; F_s, F_n, F_z = stress terms in s-, n- and z-directions, respectively; and g = acceleration due to gravity. The curvature is assumed to be sufficiently small that the metrical coefficients are approximately unity. The continuity equations for flow and sediment read

$$\frac{\partial u}{\partial s} + \frac{1}{r}\frac{\partial (vr)}{\partial n} + \frac{\partial w}{\partial z} = 0 \tag{19}$$

and

$$\frac{\partial q_s}{\partial s} + \frac{1}{r}\frac{\partial (q_n r)}{\partial n} = 0 \tag{20}$$

respectively, in which q_s, q_n = volumetric bedload transport per unit width in the s and n directions, respectively. For $r \to \infty$, Eqs. 16-20 describe the flow in straight channels.

3. Reduction of Equations

Some of the terms in the flow equations can be immediately disregarded because of their obvious smallness. In rivers, the depth of flow d is small compared with width b, so that $d/b << 1$; and radius of curvature, r, is generally larger than width. Under such conditions, v is of the order of $u(d/b)$ and w is of the order of $v(d/r)$ or $u(d/b)(d/r)$. Consequently, all terms in the governing equations containing w can be eliminated, and the stress terms are reduced to $F_s = (1/\rho)\partial\tau_s/\partial z$ and $F_n = (1/\rho)\partial\tau_n/\partial z$, where τ_s, τ_n = shear stresses in s- and n-directions respectively. As Eq. 18 is now reduced to the hydrostatic condition, the pressure terms in Eqs. 16 and 17 can be written in terms of the slope of the water surface, S in the streamwise direction and S_r in the transverse direction. It is further assumed that the flow situation is fully developed so that the $\partial/\partial s$ terms are zero. This implies that the depth-average of v is also zero.

By applying the kinematic boundary conditions at the free surface and bed, the depth-averaged equations of motion read

$$\rho g S d = \tau_{bs} + \tau_{vs} \tag{21}$$

$$\rho g S_r d = \tau_{bn} - \tau_{vn} - \rho \bar{u}^2 \frac{d}{r} \tag{22}$$

in which τ_{bs}, τ_{bn} = bed shear stresses in s- and n-directions, respectively. The effect of the submerged vanes on the flow field is accounted for by the distributed stress field (τ_{vs}, τ_{vn}) as indicated. The unknowns in these equations are $\bar{u}$, S_r, d and τ_{bn}.

An additional equation is obtained from a force balance for bedload particles on a transverse slope. The force balance includes drag, gravity, lift and friction force. At fully developed conditions the balance yields (Odgaard 1989a)

$$\frac{d(d)}{dn} = - \frac{\kappa \bar{u}}{B\sqrt{\theta \Delta g D}} \frac{\tau_{bn}}{\tau_{bs}} \tag{23}$$

in which Δ = specific weight of submerged sediment = $(\rho_s - \rho)/\rho$, ρ_s = density of sediment, D = median grain diameter, θ = critical Shields stress, and B = function of Coulomb's friction and the ratio of lift force to drag force for a bed particle. Values of B between 3 and 6 are reported by Ikeda and Nishimura (1985) and Odgaard (1989b). Herein, a value of 4 is used. For quartz sand the value of Δ is 1.65.

A fourth equation is obtained by evaluating Eq. 17 at the water surface. By eliminating S_r using Eq. 22, Eq. 17 yields

$$\rho(u_s^2 - \bar{u}^2)\frac{d}{r} + \tau_{bn} - \tau_{vn} + \left(\frac{\partial \tau_n}{\partial z}\right)_s d = 0 \tag{24}$$

in which subscript s denotes the values at the free surface. The power law relates u_s to $\bar{u}$: $u_s = \bar{u}(m+1)/m$. The last term in Eq. 24 is associated with the deformation or twisting of the velocity profile caused by the vanes or by the centrifugal acceleration acting on the flow in curved reaches of the river or by both. The centrifugal acceleration in river curves causes the faster moving surface flow to be driven toward the outer bank and the flow near the bed to be driven toward the inner bank. It is well recognized that this feature has a significant bearing on the flow and sediment processes in a channel curve. To describe the twisting of the velocity profile with a minimum amount of complexity, assumptions are made about its shape. The vertical profile of u is represented by the power law, Eq. 1, and the profile of v by a linear distribution made up of centrifugally induced and vane induced contributions,

$$v = 2(v_{vn} - v_b)\left(\frac{z}{d} - \frac{1}{2}\right) \tag{25}$$

where v_b = near-bed value of centrifugally induced transverse velocity. The vertical distribution of τ_n near the water surface is now determined as $\tau_n = \varepsilon \partial v/\partial z$. By obtaining ε from the power law and an assumed linearly distributed primary-flow shear stress, $\tau_s = \tau_{bs}(1 - z/d)$, and assuming that ε is isotropic and v given by Eq. 25, the gradient of τ_n at the water surface is

$$\left(\frac{\partial \tau_n}{\partial z}\right)_s = -\frac{2\rho\kappa^2\bar{u}}{(m+1)d}(v_{vn} - v_b) \tag{26}$$

The velocity v_b is assumed to have the same ratio to u_b as τ_{bn} to τ_{bs}, i.e.,

$$\frac{v_b}{u_b} = \frac{\tau_{bn}}{\tau_{bs}} \tag{27}$$

where, as before, $u_b = \bar{u}/k$. Thus, the ratio of v_b to τ_{bn} is the same as that of v_{vn} to τ_{vn} (Eq. 4). Eqs. 4 and 27 are now substituted into Eq. 26, which, in turn, is substituted into Eq. 24 to yield

$$\tau_{bn} = -\frac{\rho k(2m+1)(m+1)}{m^2(2m^2+m+1)}\bar{u}^2\frac{d}{r} + \tau_{vn} \tag{28}$$

With τ_{bn} calculated by this equation, $\bar{u}$ and d are fully determined by Eqs. 21 and 23. By substituting $\tau_{bs} = \rho\kappa^2\bar{u}^2/m^2$, Eqs. 21 and 23 are reduced to

$$\bar{u}^2 = \frac{m^2}{\kappa^2}\left(gSd - \frac{1}{\rho}\tau_{vs}\right) \tag{29}$$

and

$$\frac{d(d)}{dn} = -\frac{m^2}{\rho\kappa\bar{u}\ B\sqrt{\theta\Delta gD}}\ \tau_{bn} \tag{30}$$

Note that vane height H in the equations for τ_{vn} and τ_{vs} (Eqs. 5-7) is now a function of d. Without vanes, i.e., when $\tau_{vs} = \tau_{vn} = 0$, Eq. 29 is the traditional Darcy-Weisbach relation, and Eq. 28 is the equation for the transverse bed shear stress associated with the centrifugally induced secondary current in fully developed bend flow. With $\tau_{vn} = 0$ and τ_{bn} given by Eq. 27, Eq. 28 calculates a transverse velocity component that is in good agreement with measurements (Falcon 1979, Kikkawa et al. 1976, Odgaard and Bergs 1988). It is seen that if vanes are to eliminate the secondary current in fully developed bend flow, they must generate a transverse bed shear stress given by

$$\tau_{vn} = \frac{\rho k(2m+1)(m+1)}{m^2(2m^2+m+1)}\bar{u}^2\frac{d}{r} \tag{31}$$

By adopting the area averaged vane induced bed shear stress as given by Eq. 14, the design relation for this condition reads

$$\frac{NHL}{A} = \frac{2}{c_L}\frac{d}{r}G \tag{32}$$

in which $$G = \frac{k}{\lambda} \frac{(2m+1)(m+2)}{m(m+1)(2m^2+m+1)} \left(\frac{d}{H}\right)^{2/m} \tag{33}$$

This relation is similar to that developed earlier by Odgaard and Mosconi (1987).

4. Solution

Eq. 30 is solved using a finite difference scheme. The boundary condition is obtained from the continuity equation. The computation is carried out starting at the bank farthest away from the vanes. In a river curve, this is normally at the inner bank. Initially, the flow depth at the starting point is set equal to the pre-vane flow depth, and the cross-sectional distributions are calculated. If these distributions do not satisfy the boundary condition, a new starting depth is selected. The process is repeated until the boundary condition is fulfilled.

The basic vane parameters are relative vane height H_o/d_o, aspect ratio H_o/L, angle of incidence α, vane spacings δ_n and δ_s, and vane-to-bank distance δ_b. The basic flow and sediment parameters are pre-vane average flow depth d_o, velocity u_o, and resistance parameter m, the channel's width-depth ratio b/d_o and radius-width ratio r/b, and the sediment Froude number F_D, which is defined as

$$F_D = \frac{u_o}{\sqrt{gD}} \tag{34}$$

The sediment Froude number measures the mobility of the sediment. The general trend is that the vane induced changes in bed level increase with increasing value of F_D. An increase of the induced changes in bed level also occurs when relative vane height, angle of incidence, and bed resistance increase. Results of sample calculations are presented in Figures 5 and 6. The figures show depth and velocity distributions across curved and straight channels with and without vanes along one of the banks. The calculations are performed with B=4, θ=0.056, κ=0.4 and k=1. Velocities and depths are normalized with their pre-vane values, u_o and d_o.

Most design objectives can be formulated in terms of a desired change in bed elevation at the bank. To facilitate design, a number of graphs have been prepared, in Figures 7-16, showing calculated changes in flow depth at the bank as a function of the aforementioned parameters. The calculations are for a section midway between two vane arrays. One set of calculations is for curved channels and one for straight channels. For curved channels, results are shown for arrays with zero, one, two and three vanes; for straight

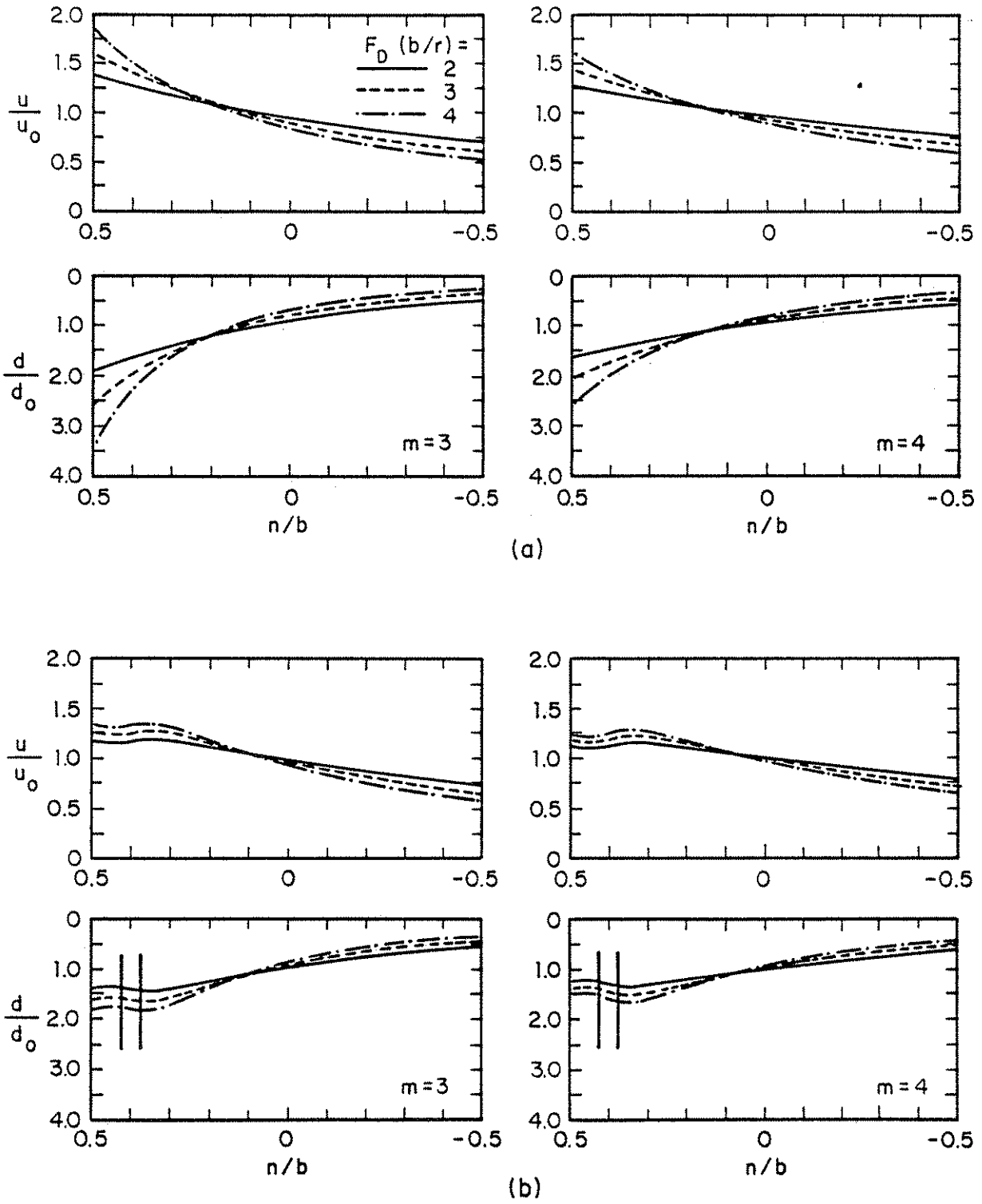

Figure 5. Calculations of depth and velocity distributions in river bend (a) without vanes and (b) with vanes, with $H_o/d_o = H_o/L = 0.3$, $\alpha = 25°$, $\delta_n = 3H_o$, $\delta_s = 15H_o$, $\delta_b = 1.5d_o$, and $d_o/b = 0.05$.

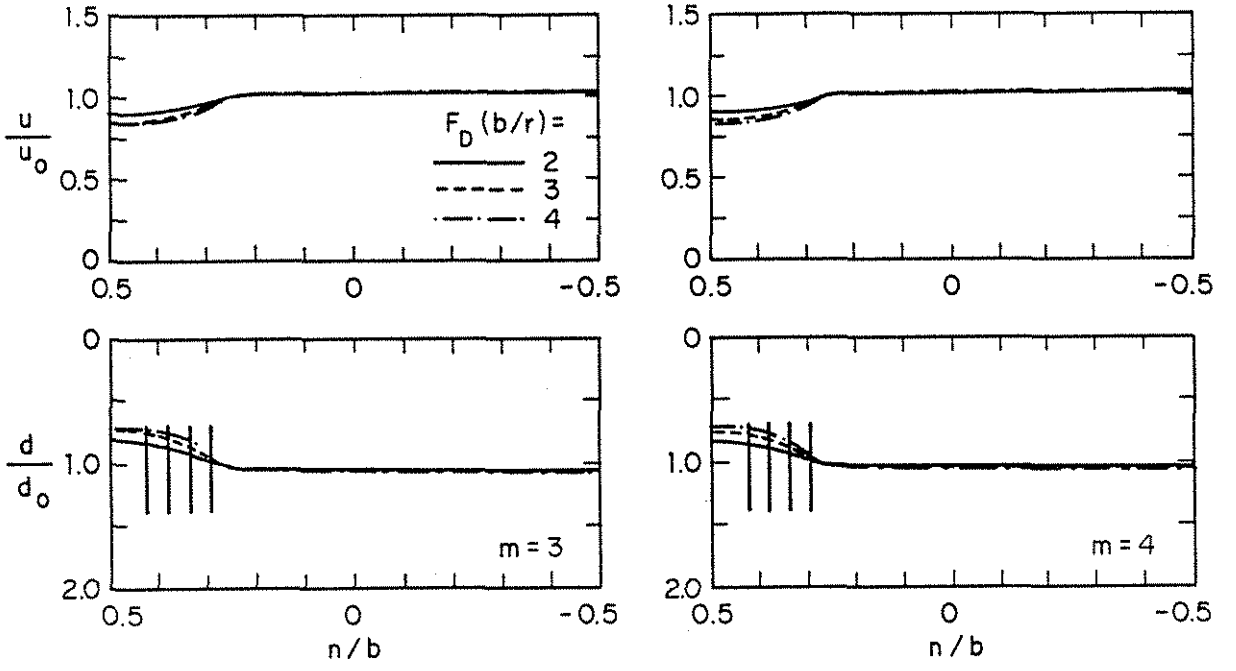

Figure 6. Calculations of depth and velocity distributions in straight channel with four-vane arrays, with $H_o/d_o = H_o/L = 0.3$, $\alpha = 25°$, $\delta_n = 3H_o$, $\delta_s = 30H_o$, $\delta_b = 1.5d_o$, and $d_o/b = 0.05$.

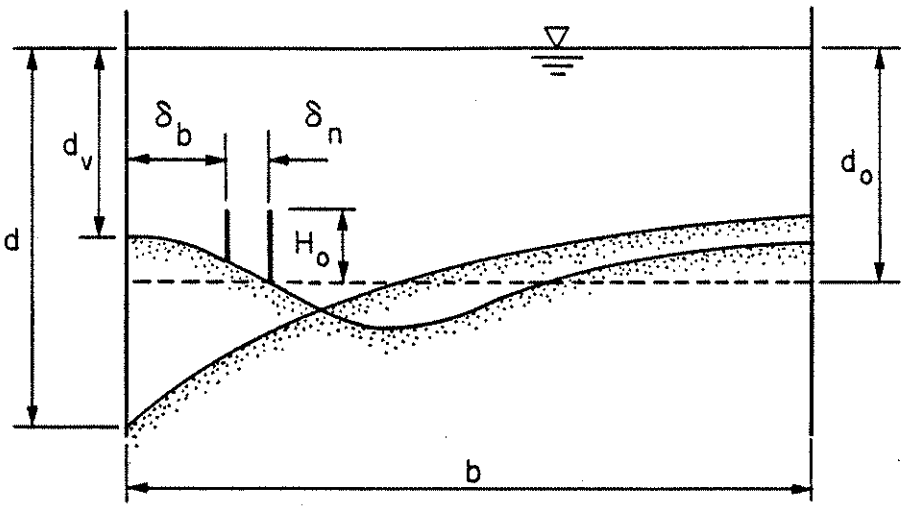

L = vane length

δ_s = longitudinal vane spacing

r = centerline radius

α = vane angle of attack

$F_D = u_o/\sqrt{gD}$

u_o = average bankfull velocity

D = sediment size

Figure 7. Key to graphs in Figures 8-16.

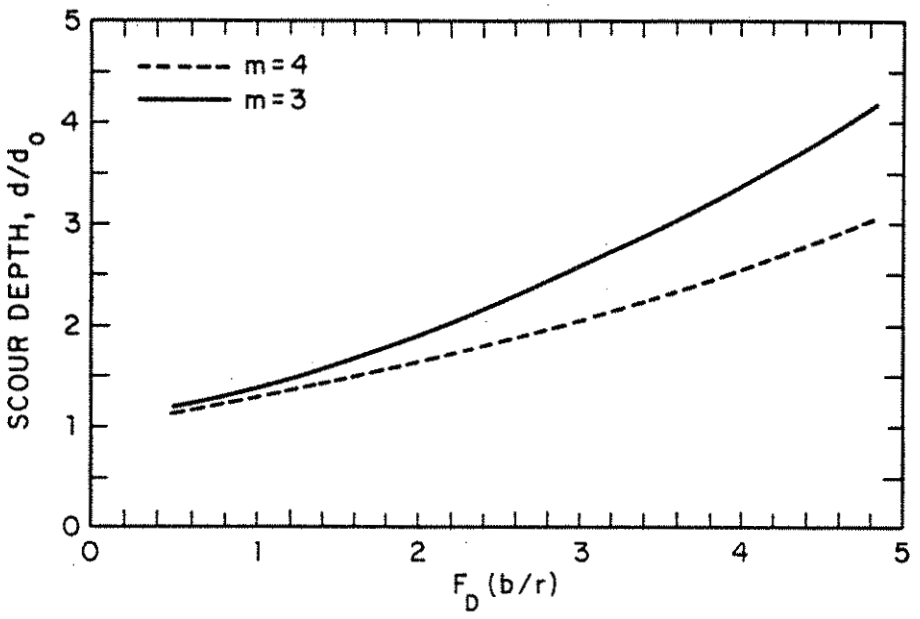

Figure 8. Scour depth at outer bank in river curve.

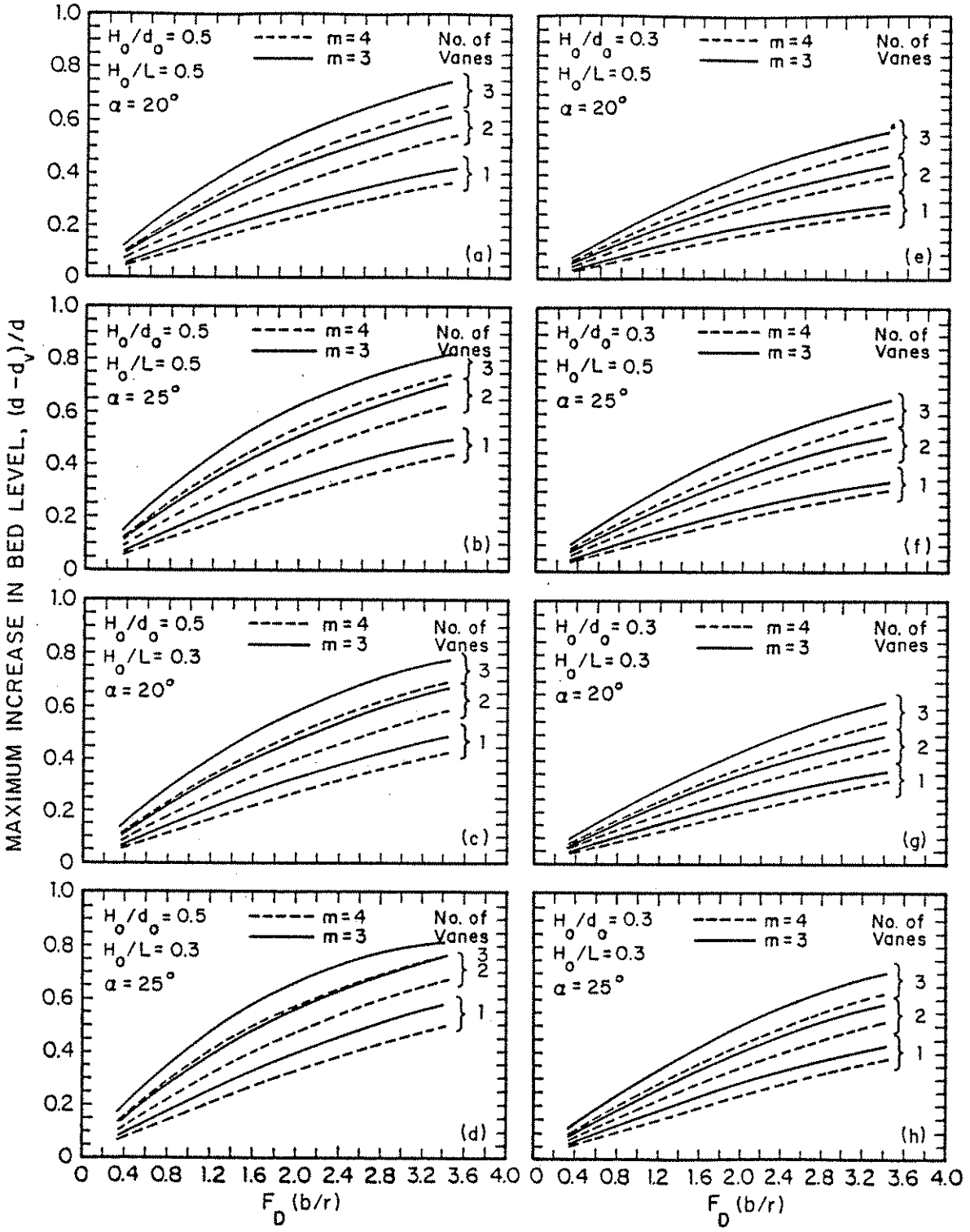

Figure 9. Computed vane induced maximum increase in bed level along outer bank in river curve. Depth-width ratio $d_o/b = 0.1$, and vane spacings $\delta_n = 2H_o$, $\delta_s = 12H_o$, and $\delta_b = 1.5\ d_o$.

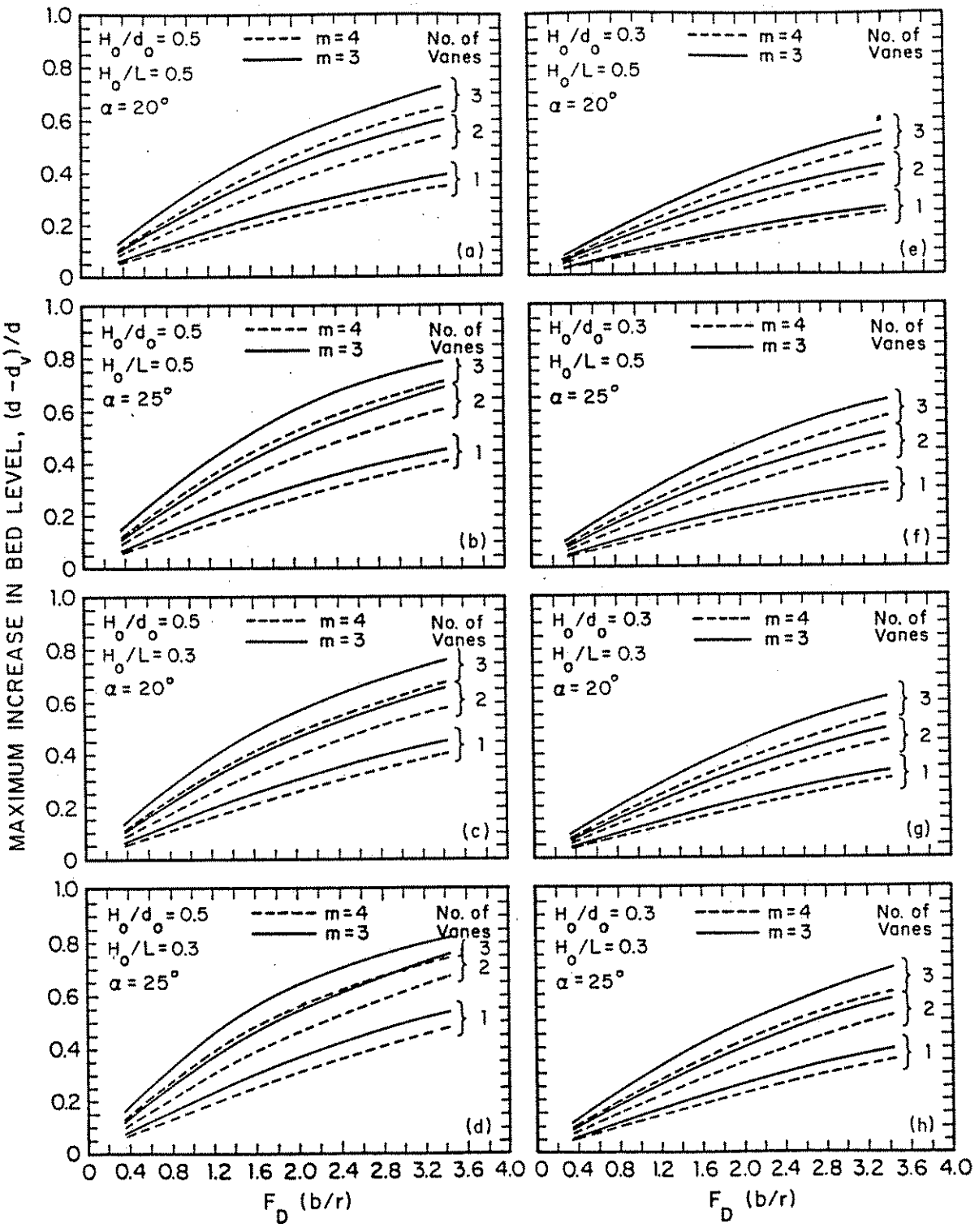

Figure 10. Computed vane induced maximum increase in bed level along outer bank in river curve. Depth-width ratio $d_o/b = 0.1$, and vane spacings $\delta_n = 3H_o$, $\delta_s = 15H_o$, and $\delta_b = 1.5\ d_o$.

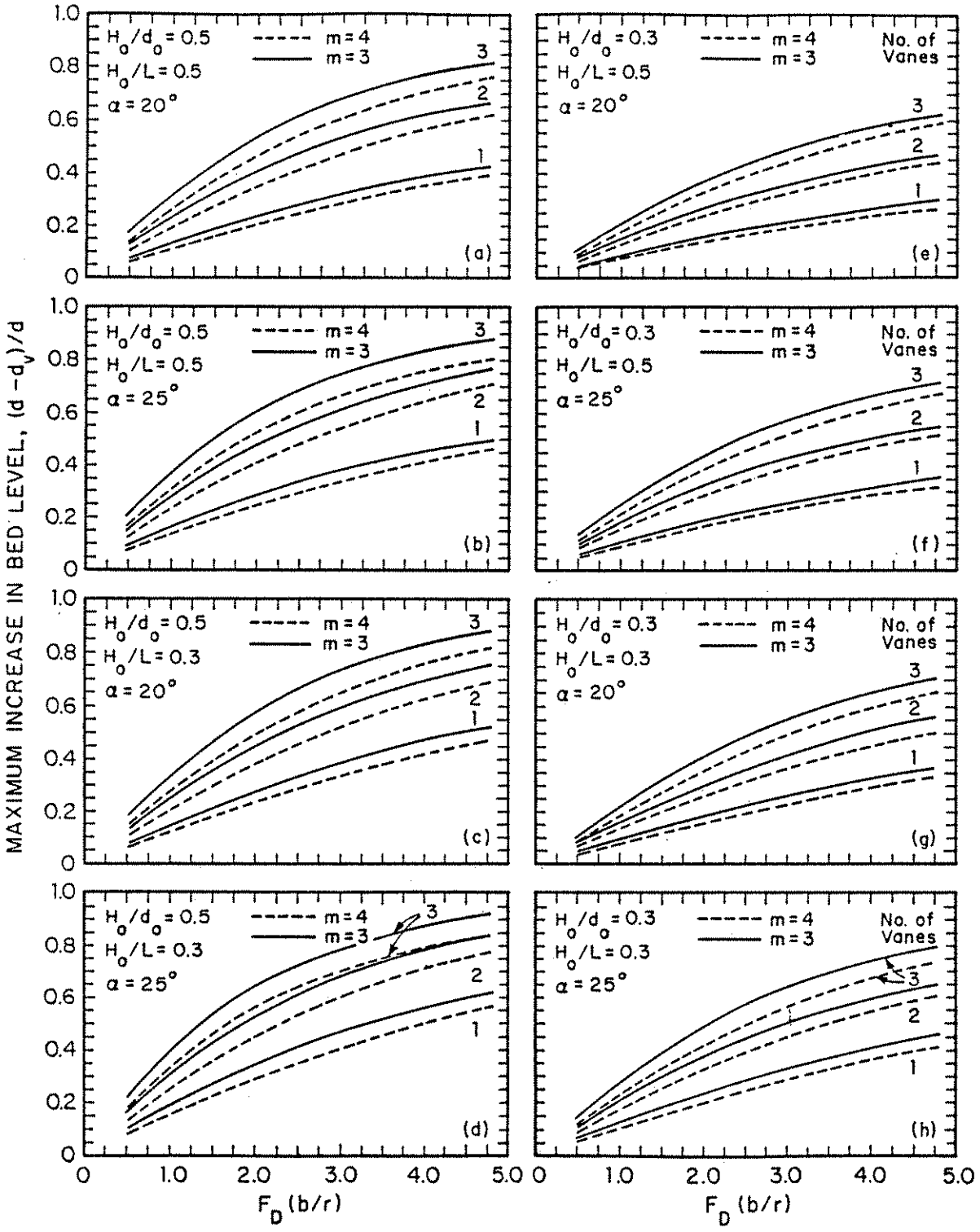

Figure 11. Computed vane induced maximum increase in bed level along outer bank in river curve. Depth-width ratio $d_o/b = 0.03$ and vane spacings $\delta_n = 3H_o$, $\delta_s = 15H_o$, and $\delta_b = 1.5d_o$.

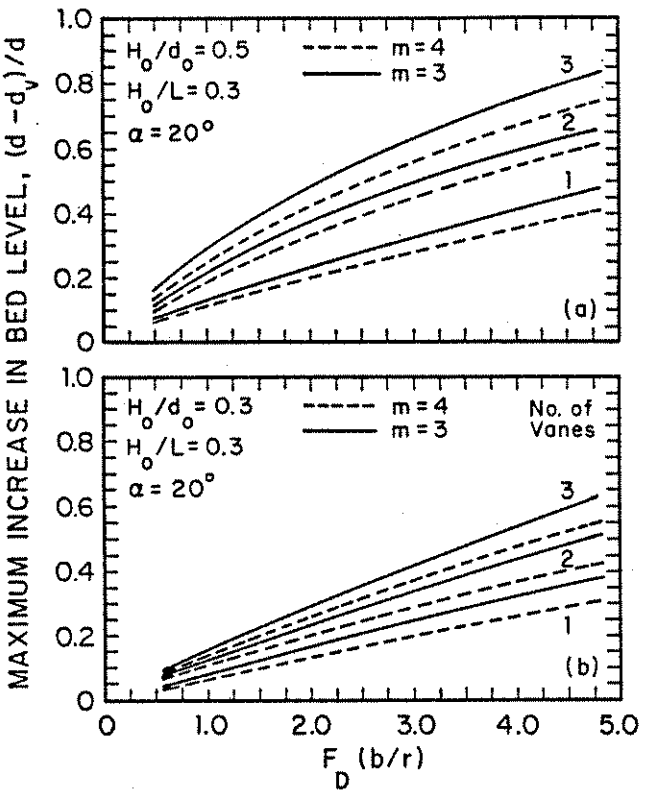

Figure 12. Computed vane induced maximum increase in bed level along outer bank in river curve. Depth-width ratio $d_o/b = 0.03$ and vane spacings $\delta_n = 3H_o$, $\delta_s = 30H_o$, and $\delta_b = 1.5d_o$.

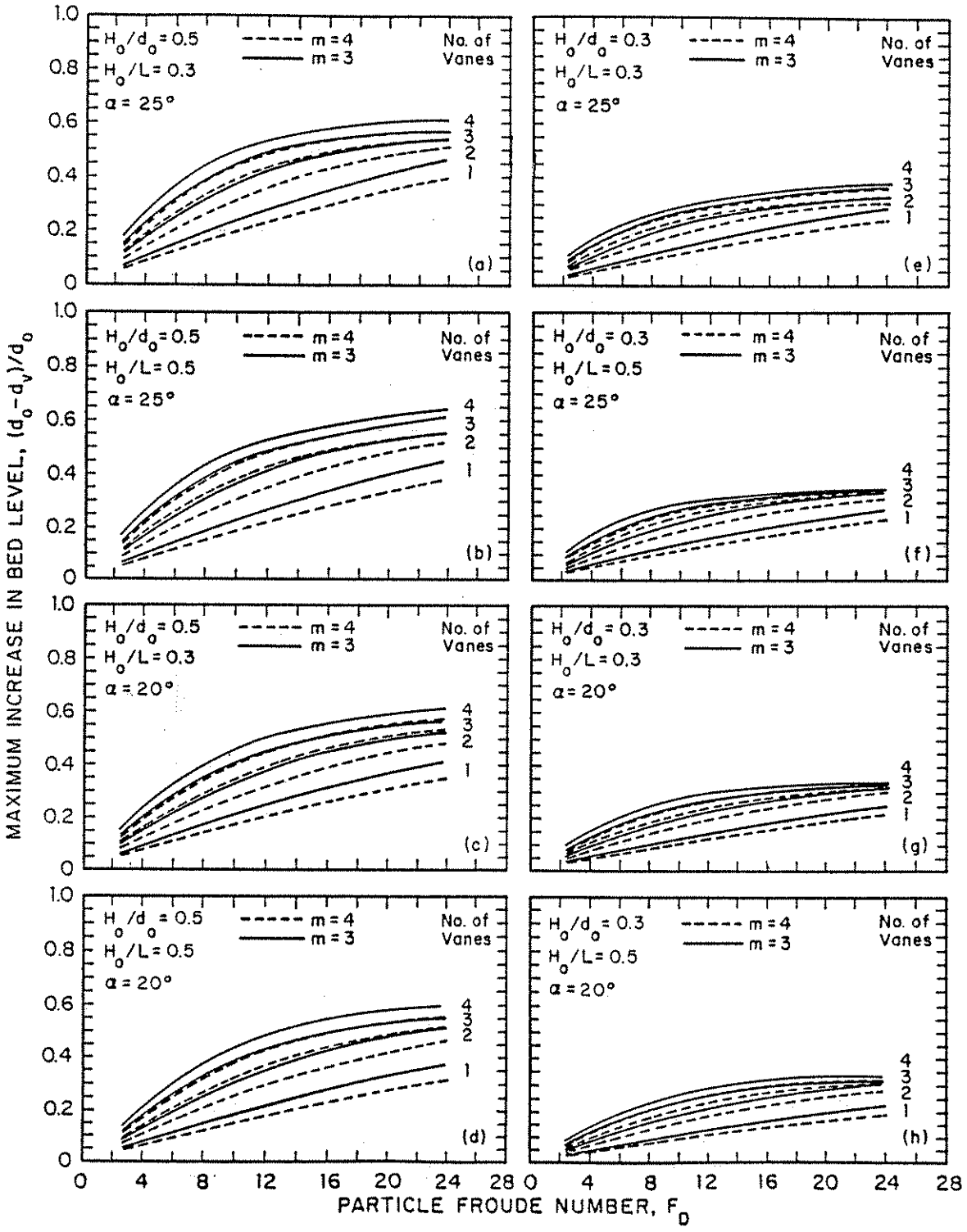

Figure 13. Computed vane induced maximum increase in bed level along bank in straight river. Depth-width ratio $d_o/b = 0.1$, and vane spacings $\delta_n = 2H_o$, $\delta_s = 12H_o$, and $\delta_b = 1.5d_o$.

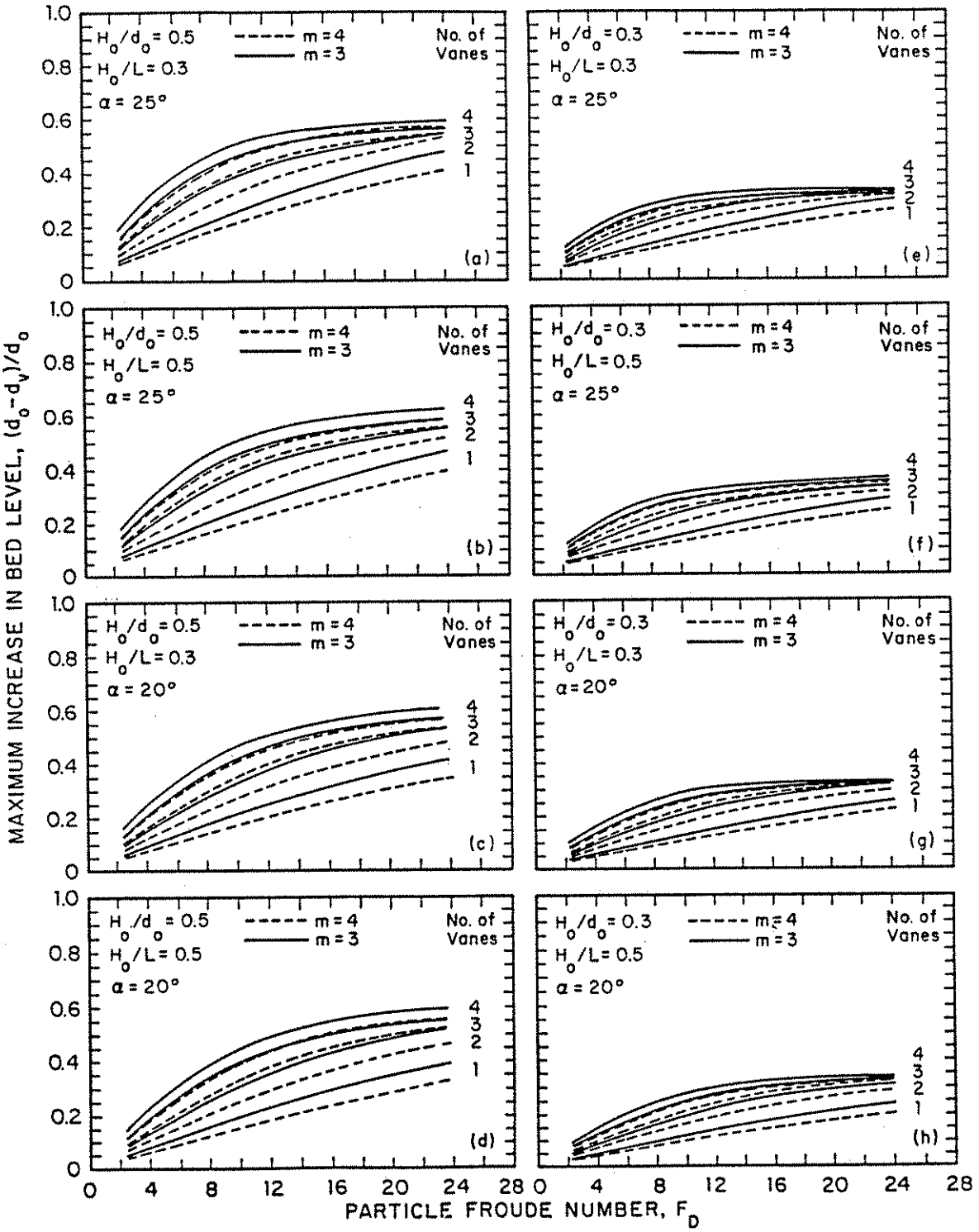

Figure 14. Computed vane induced maximum increase in bed level along bank in straight river. Depth-width ratio $d_o/b = 0.1$, and vane spacings $\delta_n = 3H_o$, $\delta_s = 15H_o$, and $\delta_b = 1.5d_o$.

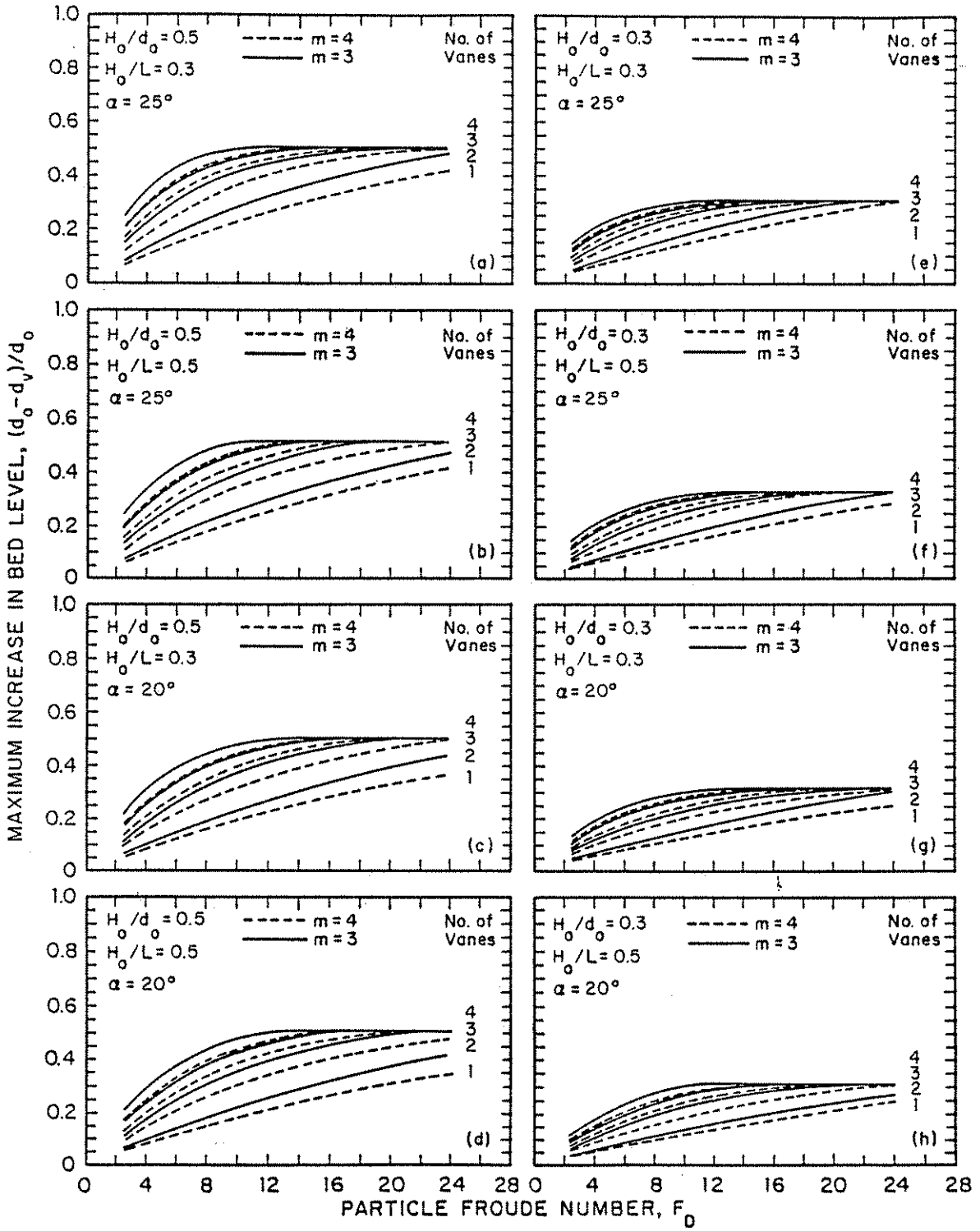

Figure 15. Computed vane induced maximum increase in bed level along bank in straight river. Depth-width ratio $d_o/b = 0.03$, and vane spacings $\delta_n = 3H_o$, $\delta_s = 15H_o$, and $\delta_b = 1.5d_o$.

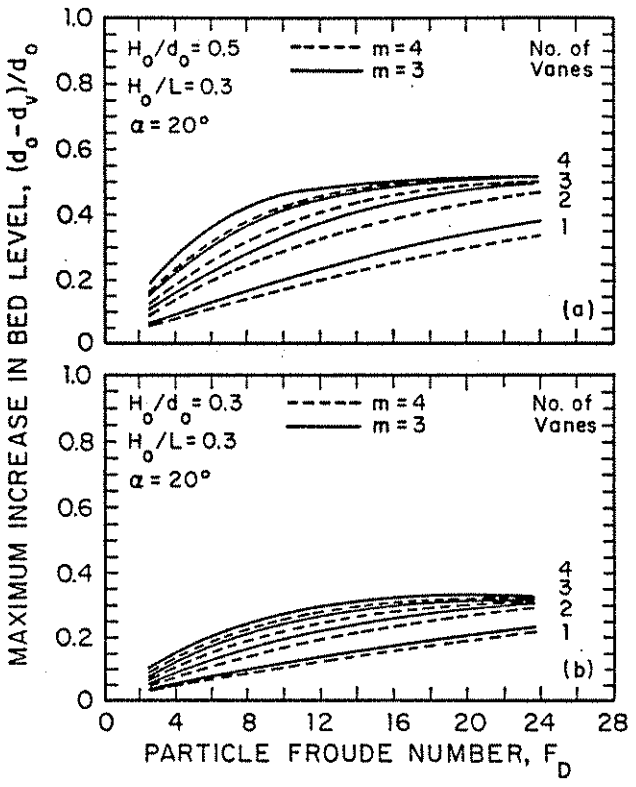

Figure 16. Computed vane induced maximum increase in bed level along bank in straight river. Depth-width ratio $d_o/b = 0.03$, and vane spacings $\delta_n = 3H_o$, $\delta_s = 30H_o$, and $\delta_b = 1.5d_o$.

channels, results are shown for arrays with one, two, three and four vanes. Each case is calculated for relative vane heights and aspect ratios of 0.3 and 0.5 and resistance parameters of m = 3 and 4. The parameter $\alpha L/H_o$ is varied between 0.7 and 1.45, F_D between 2 and 24, and $F_D b/r$ between 0.3 and 4.8. Calculations are shown for vane spacings of δ_n = $2H_o$ and $3H_o$ and $\delta_s = 12H_o$, $15H_o$, and $30H_o$, and for channels with depth-width ratios of 0.1 and 0.03.

Figure 8 shows maximum scour depth in a river curve without vanes as a function of $F_D b/r$ and m. It is seen that when $F_D b/r$ is greater than about three and m less than four, near-bank depth can be expected to be more than twice the average flow depth. For example, if $F_D(b/r) = 3.4$ and m = 3, Figure 8 yields a scour depth of $d = 2.8d_o$. The subsequent graphs in Figures 9-12 show that in order to prevent such a scour hole from forming and maintain a bed level at or above the cross-sectional average level, there must be at least three vanes in each array if relative vane height is 0.3 or at least two vanes per array if $H_o/d_o = 0.5$. In both cases, $\alpha L/H_o$ must be greater than 0.9, and $\delta_s \leq 30H_o$. For example, if $H_o/d_o = 0.3$, $H_o/L = 0.3$, $\alpha = 25°$, $\delta_n = 3H_o$, $\delta_s = 15H_o$, and $d_o/b = 0.03$, the appropriate graph is Figure 11(h). By entering this graph with $F_D(b/r) = 3.4$ and m=3, it is seen that a vane system with three vanes in each array yields $(d-d_v)/d = 0.7$. With $d = 2.8d_o$, the vane-induced depth at the bank is $0.84d_o$, or 16% less than the cross-sectional average depth d_o. More than three vanes are required in each array to raise the bed level at the bank to the top elevation of the vanes. In a straight channel, on the other hand, three vanes per array will in most cases bring the bed level to the top of the vanes provided that F_D is greater than about 15 and $\delta_s \leq 30H_o$ (Figures 13-16). Another important observation is that the induced changes in bed level decay relatively slowly in the downstream direction. By comparing, e.g., Figures 11(c) and 12(a) it is seen that by increasing the spacing δ_s from $15H_o$ to $30H_o$ in a system with 3 vanes per array, the induced change in bed level is reduced by only about 20-30%, depending on the value of $F_D(b/r)$.

Finally, it should be noted that for the vane arrays calculated above the vane induced increases in bed level are essentially independent of the channel's depth-width ratio, d_o/b, when this ratio is less than about 0.05. The depth-width ratio enters the calculations through the boundary condition (continuity equation), and when the width of the channel is large compared with the width of the vane field, the distance from the vane field to the far bank has essentially no effect on the bed level changes within the vane field.

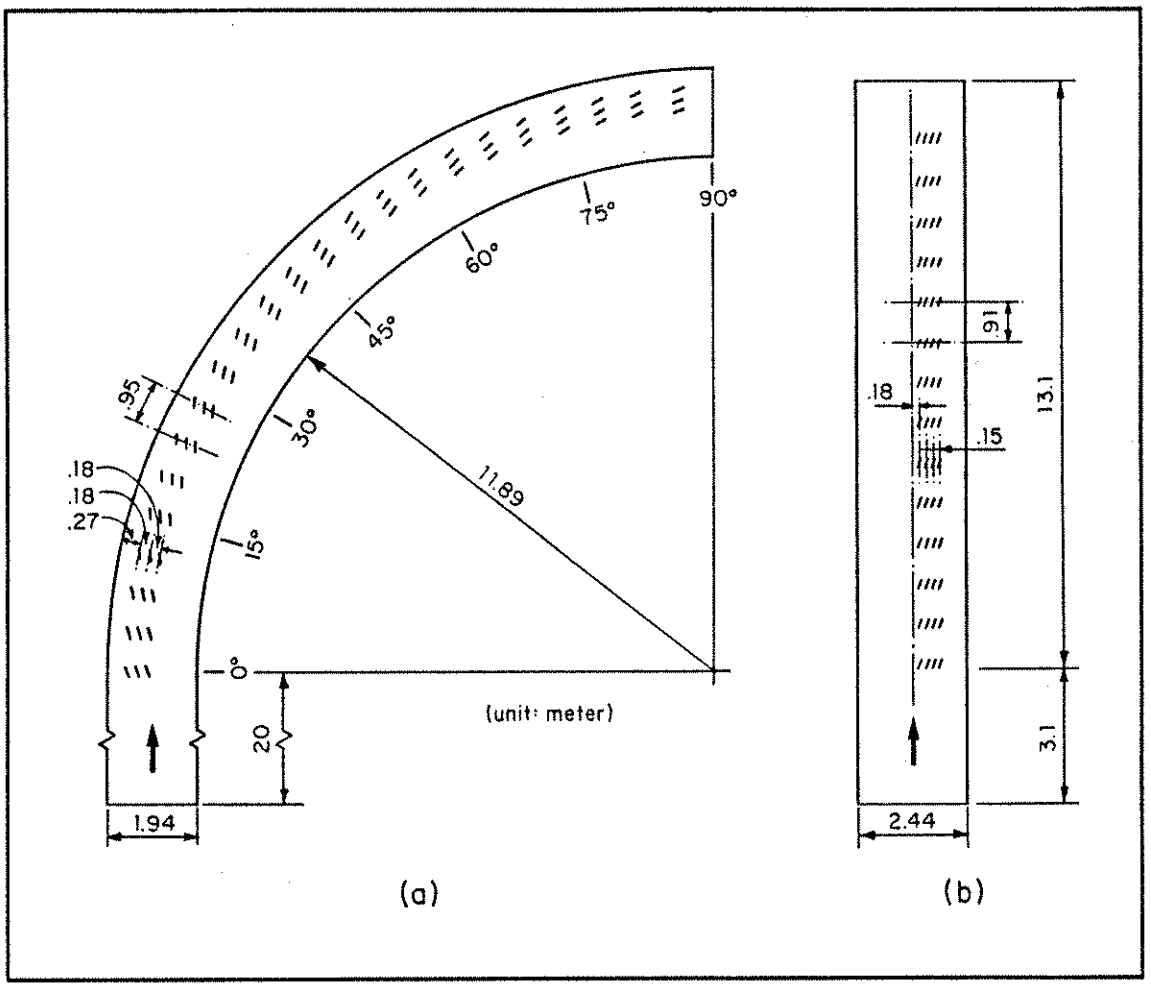

Figure 17. Layout of vane systems in (a) curved and (b) straight, recirculating laboratory flumes.

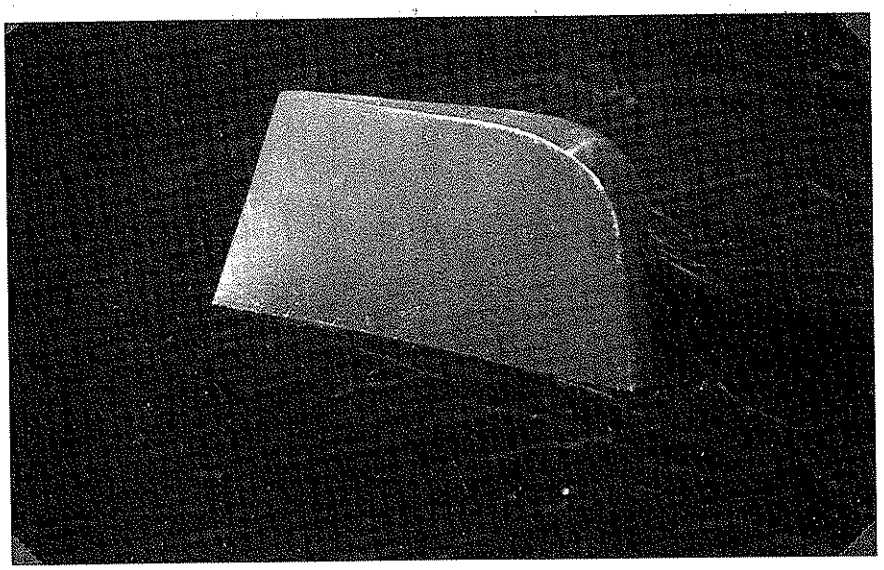

Figure 18. Model vane used in curved flume.

Table 1. Summary of Laboratory Test Conditions

Channel Plan Form	Discharge (m^3/s)	Median Particle Diameter (mm)	Centerline Average			
			Depth (m)	Velocity (m/s)	Particle Froude Number F_D	Downstream Slope of Water Surface ($x10^4$)
Curved	0.112	.41	0.16	0.39	6.2	10.1
Curved	0.137	.41	0.18	0.43	6.8	8.5
Straight	0.088	.41	0.16	0.27	4.3	3.4
Straight	0.114	.41	0.16	0.34	5.4	5.0
Straight	0.152	.41	0.18	0.40	6.3	6.4

III. VERIFICATION

1. Laboratory Tests

Tests were conducted in both a curved and a straight channel. The curved channel was a 1.94-m wide, 0.6-m deep, 13.1-m radius bend with a 20-m straight approach section (Figure 17a). The outer bank of the curve was vertical. The straight channel was 2.44 m wide, 0.6 m deep and 20 m long (Figure 17b). In both channels the bottom consisted of an approximately 14 cm thick layer of sand with a median diameter of 0.41 mm and a geometric standard deviation of 1.45. Both the water and the sediment it transported were recirculated throughout the channels and their return circuits by a centrifugal pump. The discharge was controlled by means of a butterfly valve and measured with an orifice meter. A drop gate and a weir at the downstream end of the channels were adjusted so as to produce uniform flow in the channels. Velocities were measured with a two-component electromagnetic meter, depths with a sonic sounder, and water surface elevations with a static tube. Current meter, sounder, and tube were mounted on a movable instrument carriage, which rode on rails atop the channel walls, on a traversing mechanism which enabled them to be positioned at any desired location in the channels. Positioning and data sampling were controlled from a computer on the carriage.

In the curved flume the vanes were double-curved foils with a slight twist (Figure 18). These vanes were 7.4 cm high and 15.2 cm long. They were installed in arrays with two or three vanes in each array (Figure 17a), and were angled 15° toward the bank. The tests were conducted at discharges of 0.11 m^3/s and 0.14 m^3/s. In the straight channel, the vanes were 0.8 mm thick sheet metal plates, 7.4 cm high and 15.2 cm long. These were installed in arrays with four vanes in each array and were angled 20° toward the bank (Figure 17b). In this case tests were conducted at three different discharges: 0.088 m^3/s, 0.114 m^3/s, and 0.152 m^3/s. The flow conditions are summarized in Table 1.

To obtain the prototype equivalent of these flow conditions, dimensions must be multiplied by the ratio between prototype and model dimensions, velocities by the square root of this ratio, and discharges by the ratio raised to a power of 2.5.

Figures 19 and 20 show a comparison between measured and predicted velocity and depth distributions in the curved flume with and without vanes. The agreement is good. The data points are average values in four sections located approximately 45°, 60°, 75°, and 90° into the bend. It is seen that the vanes reduced the near-bank values of depth and velocity from about 1.3 d_o and 1.2 u_o, respectively, to essentially the cross-sectional average values d_o and u_o. The photos in Figure 21 were taken after one of the tests after draining most of the water from the flume. It is evident that the vane system caused a

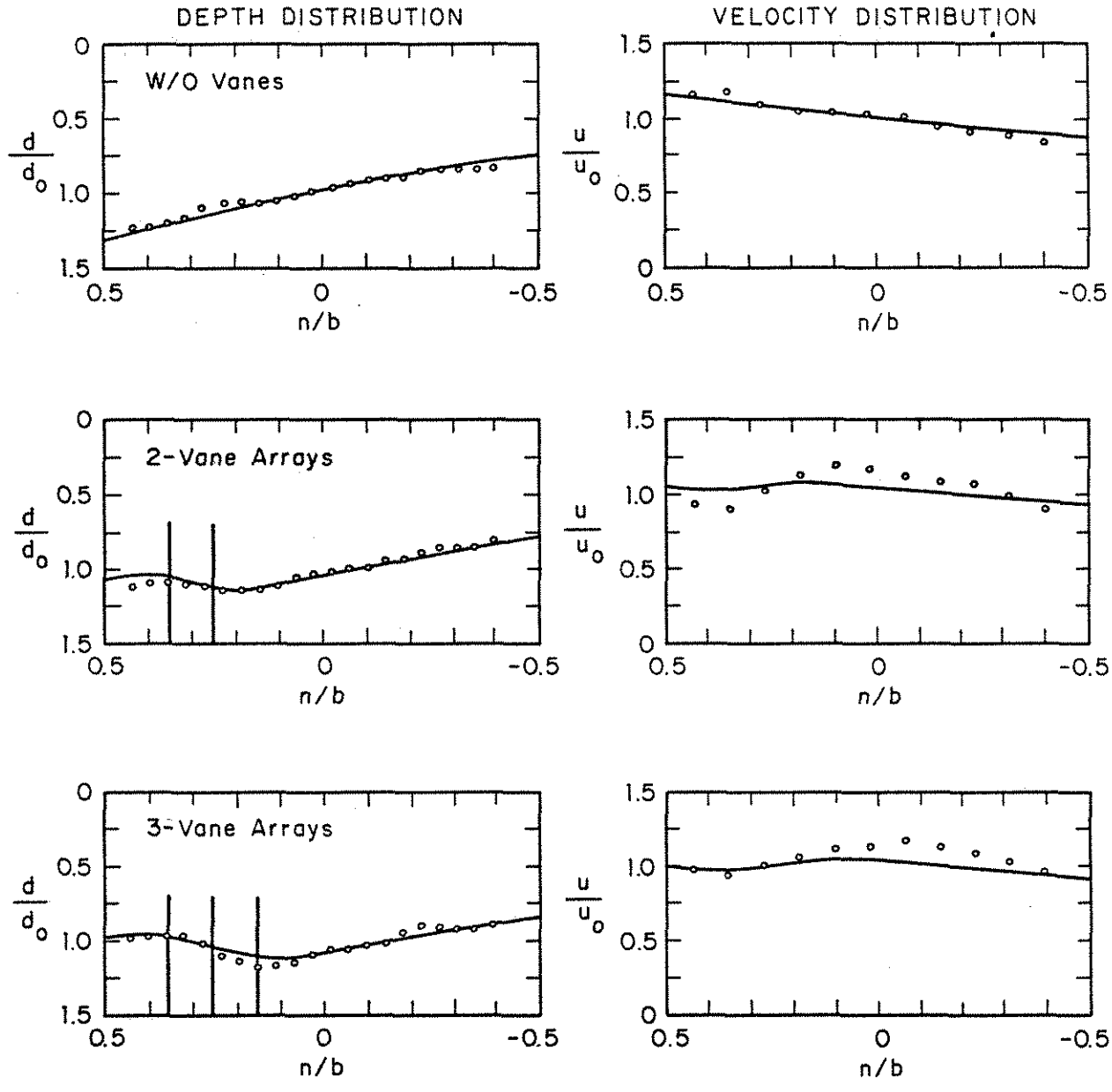

Figure 19. Comparison of measured and predicted velocity and depth distributions in the curved channel with and without vanes. Discharge = 0.11 m^3/s.

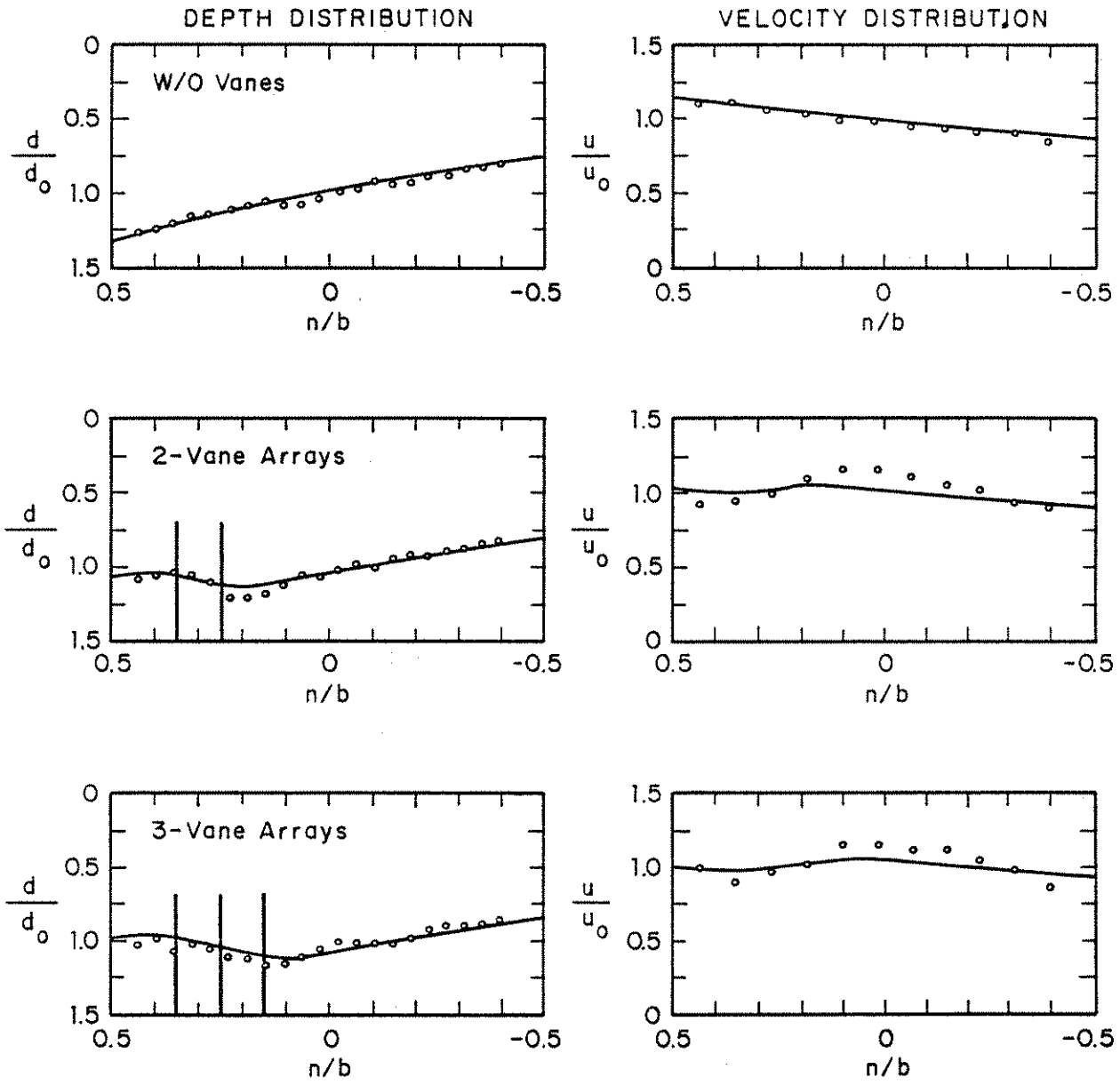

Figure 20. Comparison of measured and predicted velocity and depth distributions in the curved channel with and without vanes. Discharge = 0.14 m^3/s.

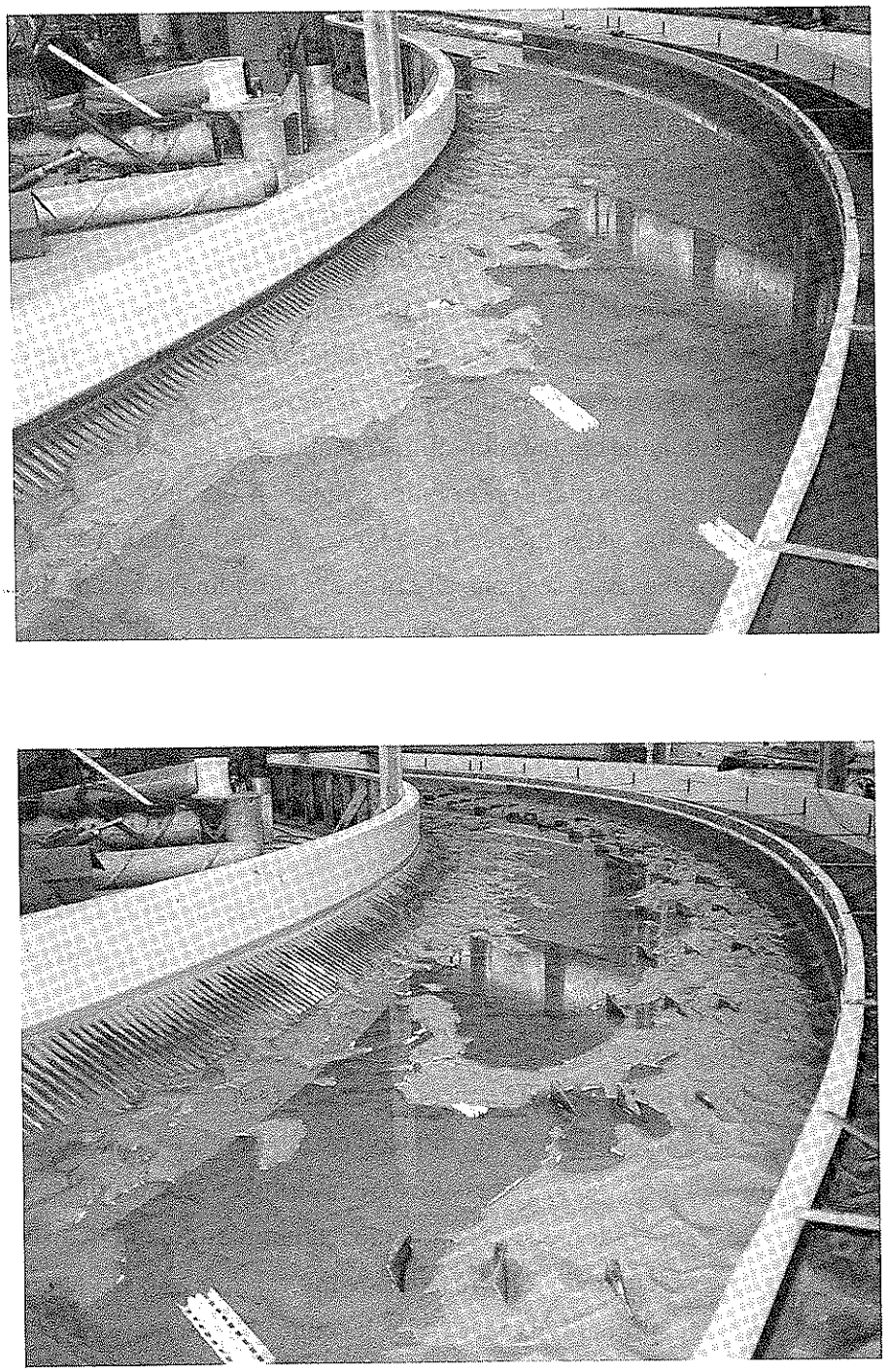

Figure 21. Upstream view of nearly drained channel bend (a) without and (b) with vanes.

considerable redistribution of sediment. By creating a wide berm along the bank the vanes effectively moved the thalweg to the center of the channel.

Figure 22 shows a comparison between measured and predicted velocity and depth distributions in the straight flume. In this case the agreement is also good. The data points are average values in four sections in the downstream half of the flume. At the largest discharge, the vanes reduced the depth near the right bank by about 50%. This caused the depth near the left bank to increase about 50%. Figure 23 is a view of the bed topography after draining most of the water from the flume. It shows the sediment accumulation in the vane field and the associated degradation of the channel outside the field.

One of the most important observations made in the tests in both the curved and straight flume is that the vane induced changes occurred without causing measurable changes of the area of the cross sections and of the longitudinal slope of the water surface. This observation is important because it implies that the vanes will not cause any changes of the stream's sediment transport capacity upstream and downstream from the vane field and therefore should not alter the overall characteristics of the stream.

Another notable observation is that the vane induced redistribution of sediment within a cross section is an irreversible process in the sense that a reduction of discharge does not lead to recovery of original distributions. A reduction in discharge does not result in a reduction in the volume of sediment accumulated in the vane field because at the lower discharge the sediment transport capacity in the vane field is too low to remove the sediment that accumulated at the higher discharge.

Finally, it must be recognized that the relatively good agreement between theory and data may be somewhat deceptive. The theory of vanes is developed for non-separated flow around the vanes. The magnitude of the induced circulation is calculated by assuming that the rear stagnation point on the low pressure side is shifted to the trailing edge of the vane. In reality, some flow separation occurs, and induced circulation and bed shear stresses are different from those calculated. The reason for the relatively good agreement between theory and experiments probably is that while it reduces the transverse component of the induced bed shear stress, flow separation increases the streamwise component by a comparable amount. In this case, the difference between theory and data is not in the total amount of aggradation but in the transverse slope of the aggraded bed, which obviously is difficult to measure.

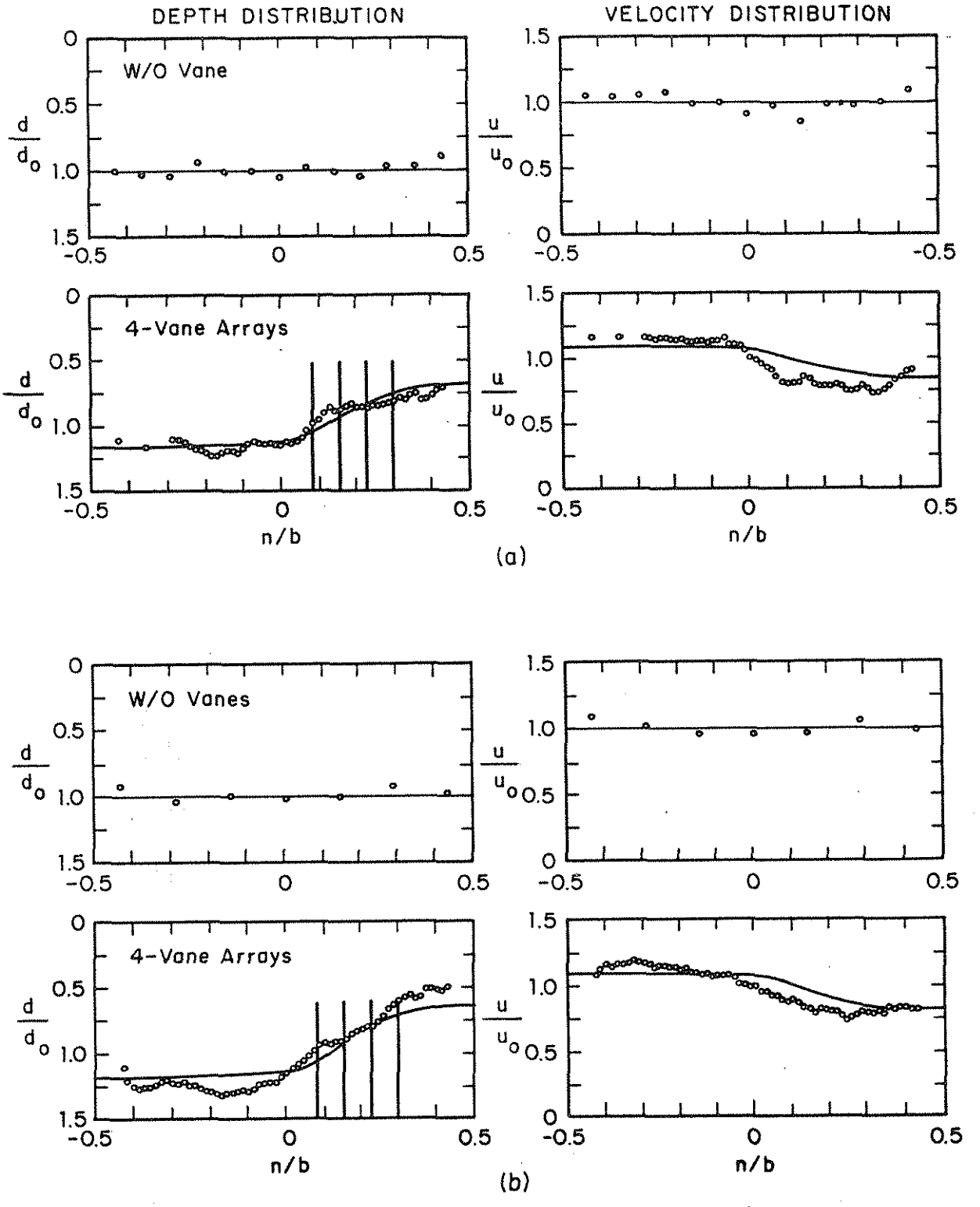

Figure 22. Comparison of measured and predicted velocity and depth distributions in straight channel with and without vanes (a) discharge = 0.114 m^3/s; (b) discharge = 0.152 m^3/s.

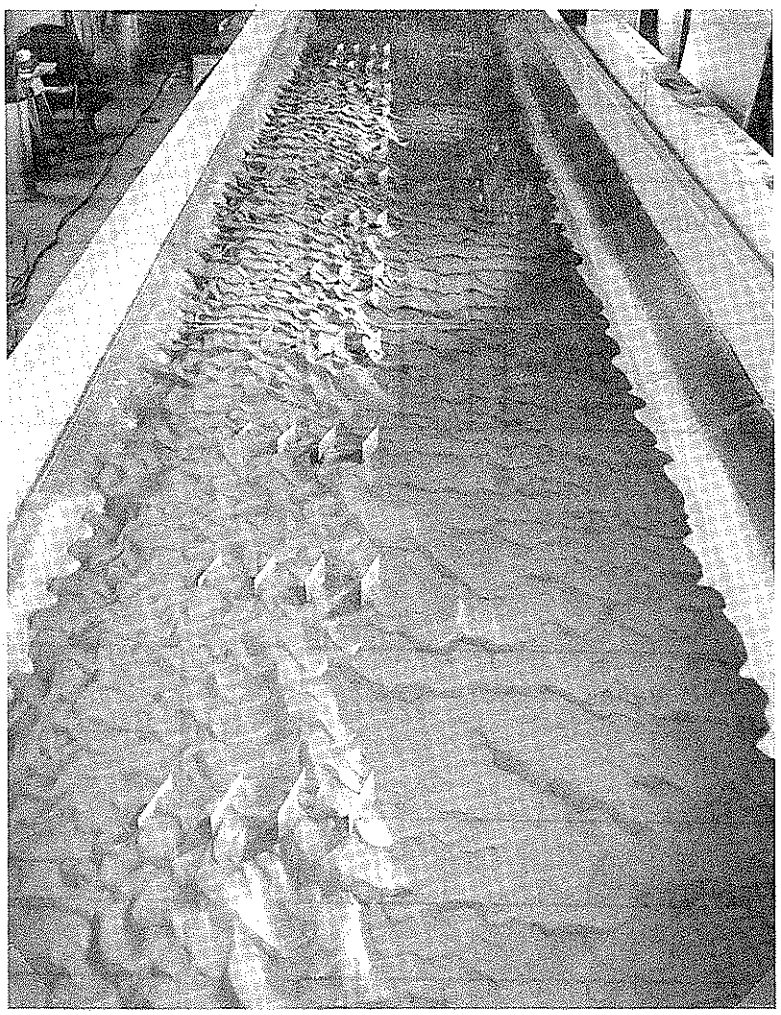

Figure 23. Upstream view of nearly drained, straight channel with vanes.

2. Field Tests

Several field installations are in place. As mentioned earlier, the first installation for preventing bank erosion in a river curve was in East Nishnabotna River, Iowa. This installation is performing satisfactorily. Design, construction and performance evaluation were described earlier by Odgaard and Mosconi (1987), and the preceding laboratory tests by Odgaard and Lee (1984). Figure 24 shows a comparison between measured and predicted bankfull depth distributions at midbend in the East Nishnabotna bend. The agreement is good. Field tests are also underway in Kuro River, Japan. These tests were preceded by laboratory tests at the Public Works Research Institute of the Japan Ministry of Construction. All results are very good. The Japanese laboratory and field tests are described by Fukuoka (1989) and Fukuoka and Watanabe (1989). Banks in Wapsipinicon and Cedar Rivers in Iowa now also are being protected with vanes (Odgaard and DeWitt 1988).

The effectiveness of submerged vanes in ameliorating prototype shoaling problems is demonstrated at a highway crossing of West Fork Cedar River in Butler County, Iowa. The problems at this site developed following a straightening and widening of the river at the time of construction of the bridge (1970). Figure 25 shows the excavation plan for the project (Butler County Project No. S-1024(6)-50-12, dated 1969). The bridge is a 150-m long, 9-m wide, six-span, I-beam bridge with the road surface about 5 m above the low-flow streambed. The top width and bankfull depth of the river upstream from the excavation are 30-40 m and 1.9 - 2.1 m, respectively. The bed material is sand with a median particle diameter of about 0.5 mm. Annual mean flow in the river is about 14 m^3/s and bankfull flow about 100 m^3/s. A 10-m wide channel running parallel with the roadway connects the old channel with the new. Aerial photos indicate that the new channel was constructed as shown on the excavation plan. The channel parallel with the road, however, was constructed somewhat closer to the roadway than shown on the plan.

By 1984, a considerable portion of the excavation upstream from the bridge had filled in and become vegetated. Figure 26 shows the 1984 bankline and a sandbar which subsequently developed along the left bank. The sandbar occupied four of the six spans, and it caused the flow to be thrown toward the right bridge abutment where it undermined and eroded the bank. Annual dredging was necessary because the sand bar grew in size after each storm. It was clear from aerial photos that the bar formed as part of the river's adjustment to the 1970 channel straightening, which essentially eliminated two meanders and shortened the channel segment by 482 m (from 1,189 m to 707 m). The straightening resulted in a 69% increase in the local channel slope, from 0.00049 to 0.00083.

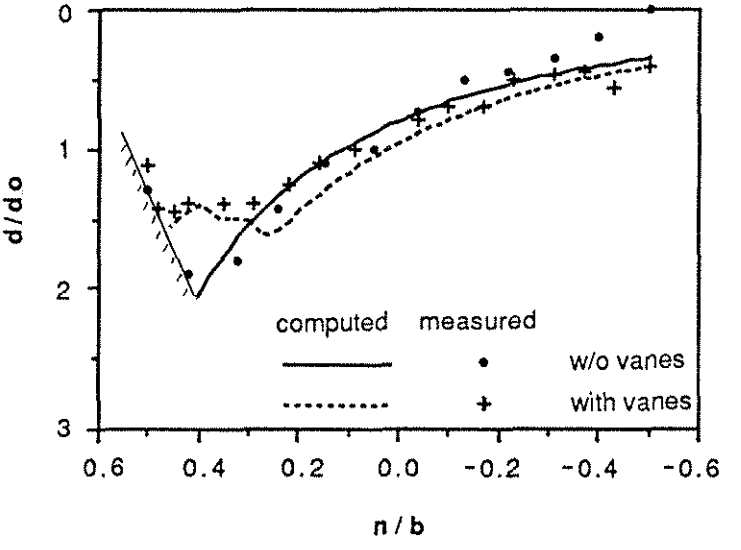

Figure 24. Comparison of measured and predicted bankfull depth distributions in bend of East Nishnabotna River, Iowa, with and without vanes.

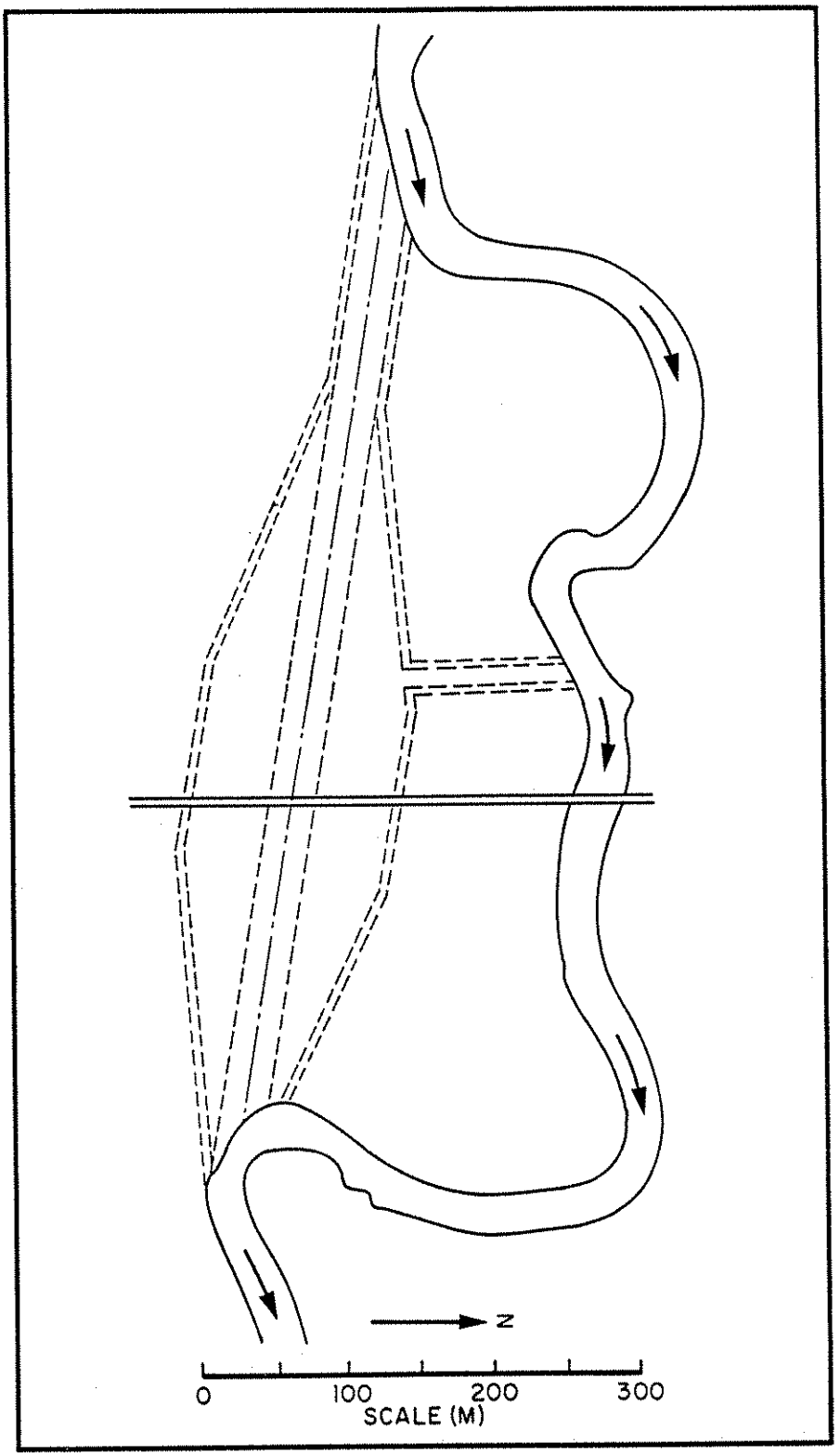

Figure 25. Excavation plan for West Fork Cedar River channel straightening.

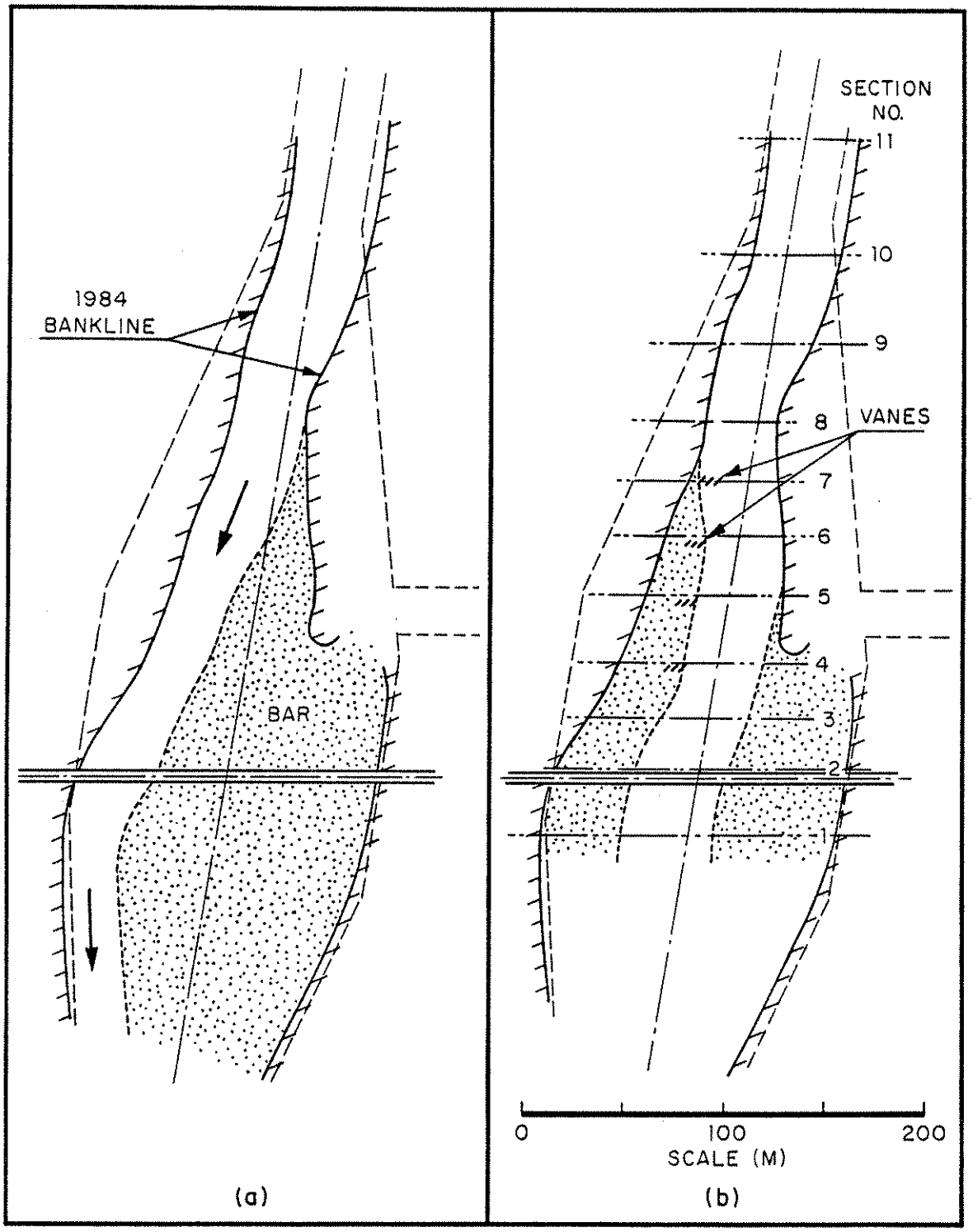

Figure 26. Plan of West Fork Cedar River bridge crossing (a) prior to vane installation in 1984 and (b) in 1989 five years after vane installation. Plan (b) shows location of vanes and survey sections.

A system of 12 vanes was installed in the summer of 1984. The layout is shown in Figure 26b. Each vane consists of vertical sheet piles driven into the streambed and aligned at a 30° angle with the main channel (Figure 27). With this angle, the vanes are at about 20° with the 1984 mean flow direction, which is indicated by the arrows in Figure 26a. Each sheet piling was 3.7 m long and its top elevation was 0.6 m above the streambed. The vane system was designed to cause flow depth and velocity to decrease along the right bank and increase along the centerline. As seen in Figure 28, the system has accomplished this. A permanent, protective berm now is seen along the bank that was previously being eroded (about 450 m). In fact, the vanes are now maintaining a cross-sectional bed profile similar to that designed when the bridge was constructed. Installation cost was $5,000, and, so far, maintenance has not been necessary. Six of the 12 vanes are now permanently covered with sand and vegetation (Figures 29 and 30).

A field survey was conducted on August 22, 1989, with the purpose of quantifying the induced changes in bed topography. The flow in the river was about 0.3 m^3/s on that day. Bed profiles were taken in 10 sections upstream from the bridge and in one section downstream from the bridge. The location of the sections are indicated in Figure 26b, and the profiles are shown in Figure 31. It is seen that the vanes have caused the bed to aggrade by 0.6 to 1.0 m within the vane controlled area, which is essentially the old, pre-vane low flow channel. The aggradation, or berm, starts about 10 m downstream from the first vane array and continues downstream past Section No. 1. The width of the berm is 20-30 m. Between Sections 7 and 1, the vane induced aggradation amounts to about 3,300 m^3 or 276 m^3 per vane. The aggradation along the bank downstream from Section 1 appears to be of the same order of magnitude.

It is noted that the aggradation straight downstream from the last vane array is decreased and at Section 3 is less than 0.5 m. At this section, and at downstream sections, the major aggradation occurred toward the right bank. The decrease in aggradation straight downstream from the last vane array is due to the decay of vane induced circulation. The reason for the enhanced aggradation along the bank downstream from the vanes is that the vanes have caused the main current to be shifted toward the central portion of the channel so that the velocities along the bank are now considerably lower than before.

The vane induced aggradation is somewhat better than predicted. At bankfull flow, the velocity at Sections 4 and 5 is about 0.9 m/s yielding a particle Froude number of F_D = 13. With a friction parameter of m = 3-4, a vane height to water depth ratio of H_o/d_o = 0.3, and aspect ratio of $H_o/L \simeq 0.2$, Figure 16 yields $d_o - d_v$ = 0.6 m. The reason for the enhanced aggradation is probably the vegetation, which increases flow resistance on the berm and causes the sediment transport capacity to decrease below that predicted by the

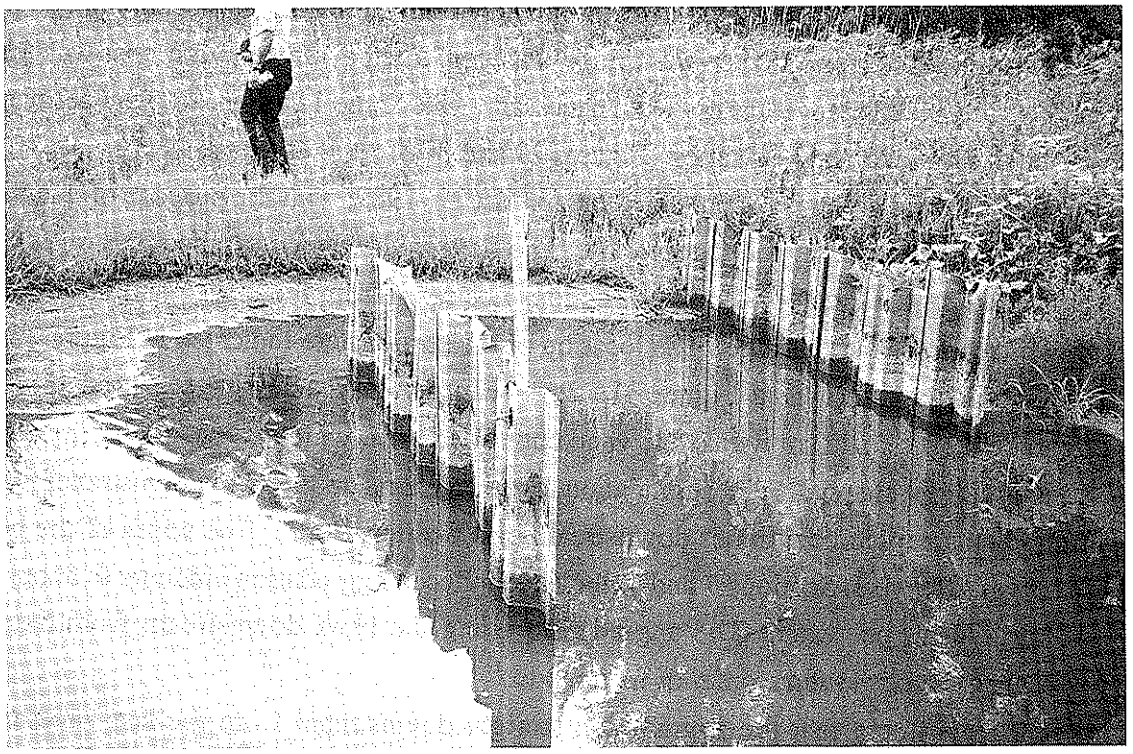

Figure 27. Downstream view of sheet pile vanes used at the West Fork Cedar River bridge crossing. August 1989.

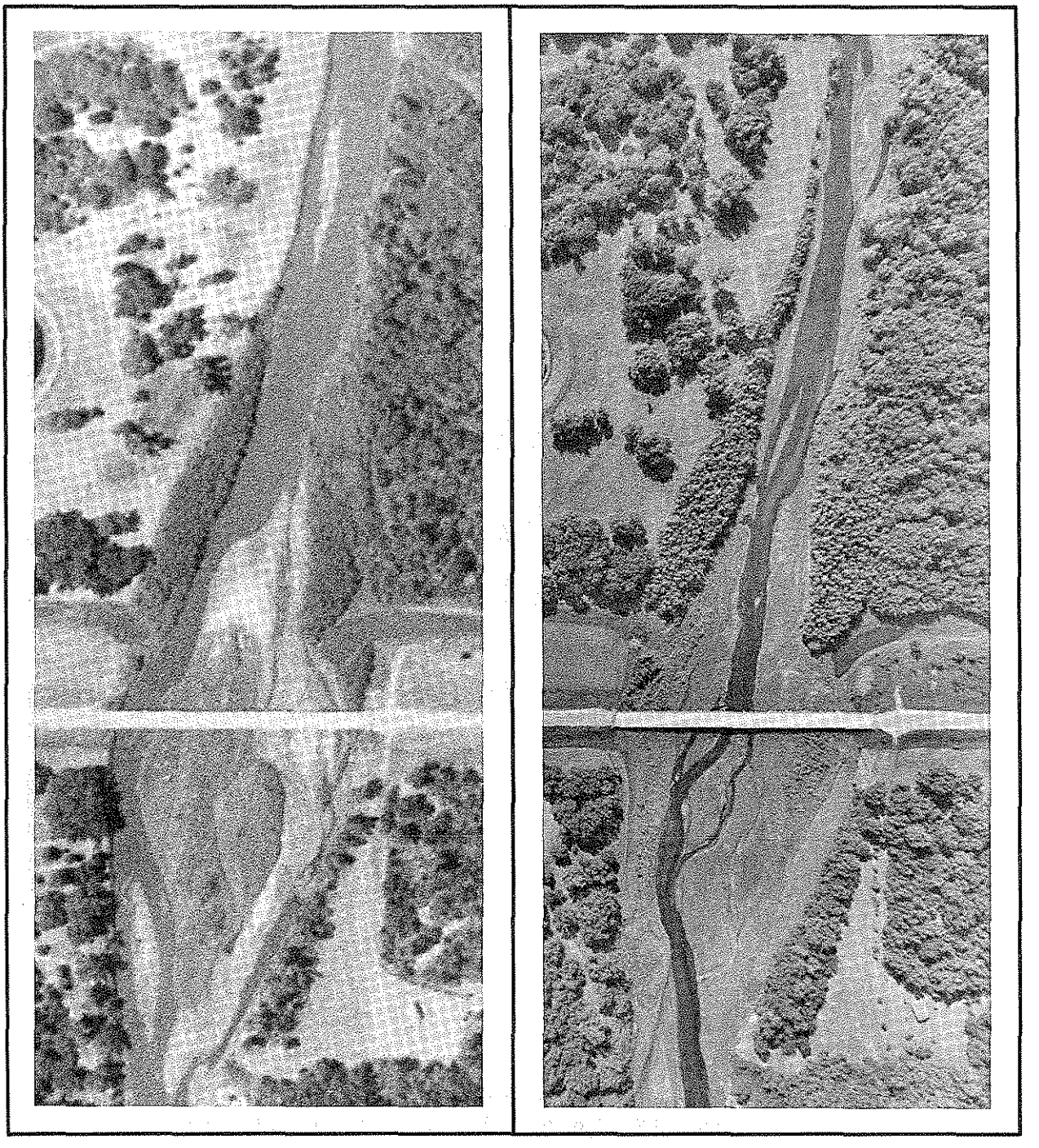

Figure 28. Aerial photos of West Fork Cedar River bridge crossing (left) prior to vane installation in 1984, and (right) in 1989, five years after vane installation.

Figure 29. View downstream toward the Butler County bridge, August 1989. The bank that was eroding prior to vane installation is by the tree line to the right in the photo.

Figure 30. View upstream from the Butler County bridge , August 1989. The bank that was eroding prior to vane installation is by the tree line to the left in the photo.

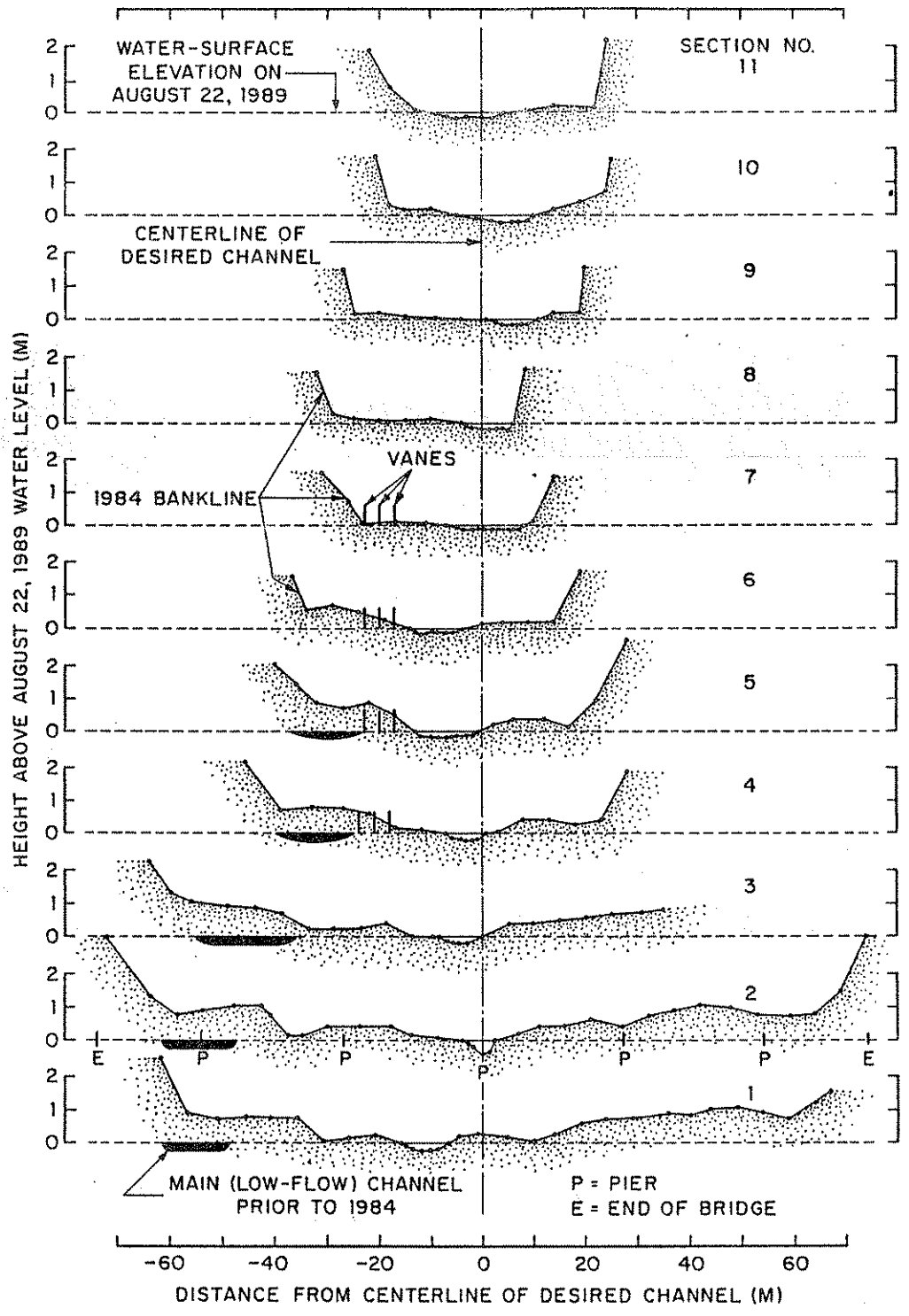

Figure 31. Cross sections in West Fork Cedar River measured on August 22, 1989.

theory. Because of the steadily increasing vegetation on the berms, it is expected that the aggradation process will continue somewhat.

A final comparison between measured and predicted results is seen in Figure 32. Compared are the maximum vane induced depth change at the bank in the laboratory and field channels. It is apparent that the predictor developed herein is good for both laboratory and field conditions.

IV. DESIGN PROCEDURE

The design procedure can best be described with reference to the solutions presented in Figures 8 - 16. The procedure is essentially a back calculation. The desired bed topography is the main input, and vane layout and design are the outputs. Because the ultimate shaping of the channel cross section occurs during and immediately after high flows, data for bankfull flow are used in the design. The steps are as follows:

(1) Determine bankfull-flow variables: average width b, depth d_o, velocity u_o slope S, radius of curvature r, and median grain diameter of the bed material D.

(2) Calculate m, F_D, d_o/b and b/r.

(3) Define desired maximum change of depth to be achieved by the vane system, $d-d_v$ or d_o-d_v, where d = maximum depth without vanes and d_v = corresponding depth with vanes.

(4) Select vane dimensions H_o and L, and angle of attack α; and calculate H_o/d_o and H_o/L.

(5) Enter appropriate graph and determine (read) the number of vanes per array required to obtain the desired value of $(d-d_v)$ or (d_o-d_v). Note that the objective can often be met with different combinations of array spacing δ_s and number of vanes per array.

(6) Select other vane dimensions and enter the appropriate graphs to determine if the objective can be met with more favorable designs and layouts.

The following numerical examples illustrate the procedure. The river data used are typical for many rivers in Iowa and the Midwest.

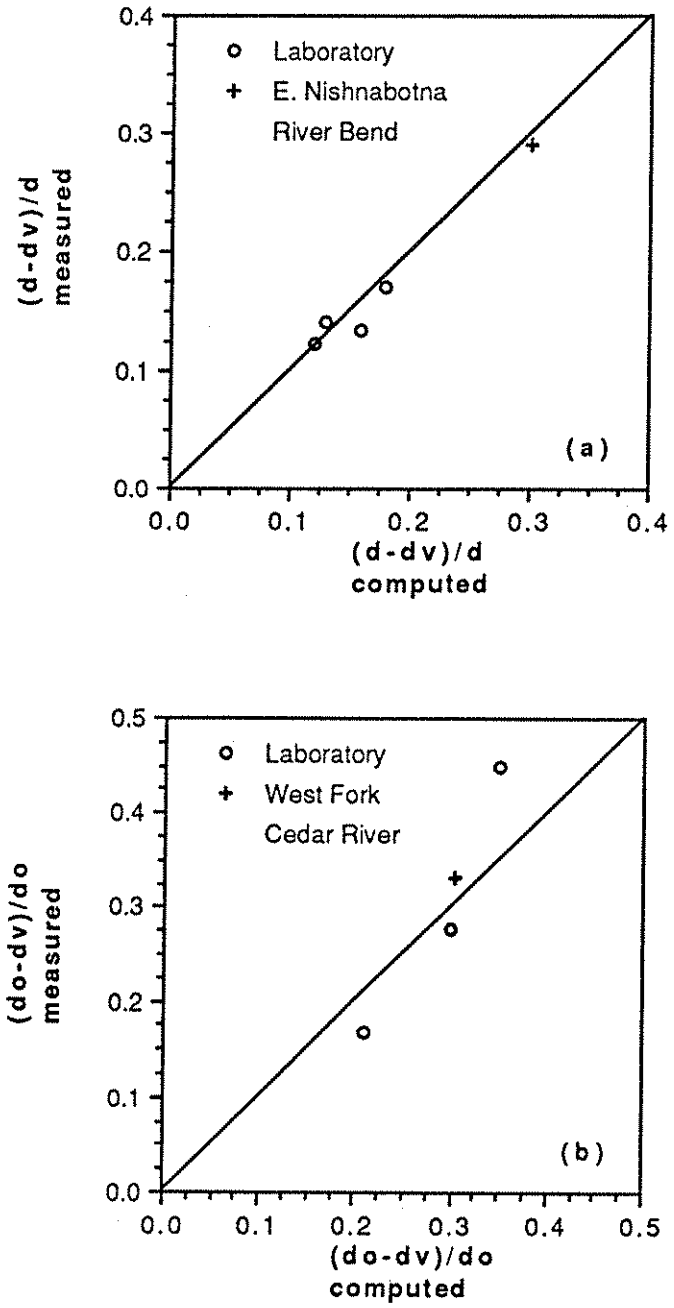

Figure 32. Comparison of measured and predicted vane induced decrease in flow depth at the bank.

1. Numerical Example 1

The conveyance of a bridge waterway is reduced due to a sand bar which has formed in the central portion of the channel. The bar has caused the main channel to move toward the abutments where it is causing undermining and scour. At bankfull flow, average width, depth, slope and velocity are $b = 50$ m, $d_o = 2$ m, $S = 0.00075$, and $u_o = 1.2$ m/s. The bed material is sand with a median grain diameter of $D = 0.6$ mm.

The channel's resistance parameter is $m = \kappa u_o / \sqrt{gSd} = (0.4)(1.2)/\sqrt{(9.81)(0.00075)(2)} = 4.0$, which corresponds to a Darcy-Weisbach friction factor of $f = 8\kappa^2/m^2 = 0.08$. The sediment Froude number is $F_D = u_o/\sqrt{gD} = (1.2)/\sqrt{(9.81)(0.6 \times 10^{-3})} = 15.6$.

A vane system is to be designed to modify the flow field and create and maintain a depth distribution that permits the flow to pass the bridge without endangering the structure. To make the cross section stable, the vanes should be laid out to promote deposition of sediment on berms along the sides of the channel. The berms must be sufficiently high that the bed level in the central portion of the channel at all stages remains below the average bed level. To ensure that this is accomplished, the flow depth on the berms, d_v, must at all stages be less than the average flow depth in the channel d_o. Berms of width b_1 with a top elevation of $(d_o - d_v)$ above the average bed level will create a deepening of the central portion of the channel of the order of

$$d_c - d_o = \frac{2b_1}{b - 2b_1}(d_o - d_v) \tag{35}$$

in which d_c = flow depth in the central portion of the channel.

A reasonable height of the berm will be 0.2-0.3 times flow depth and the width of the berm 10-20% of bankfull channel width. By creating an 0.6-m high, 8-m wide berm along each side of the channel, the central deepening will be

$$d_c - d_o = \frac{(2)(8)}{(50) - (2)(8)}\ (0.6) = 0.3 \text{ m} \tag{36}$$

This should be sufficient to ensure that the river maintains a central approach to the bridge.

The channel's depth-width ratio is $d_o/b = (2)/(50) = 0.04$. This is sufficiently small that this parameter does not play a role. The appropriate graphs are those prepared with $d_o/b = 0.03$, i.e., Figures 15 and 16.

If the vane height is selected to be $H_o = 0.3\ d_o = 0.6$ m, the lateral spacing between the vanes should be of the order of $\delta_n = 3\ H_o = 1.8$ m or less. With $\delta_n = 1.8$ m, each array

must contain four vanes. The vane-to-bank distance will then be $\delta_b = (8) - (3)(1.8) = 2.6$ m, which is acceptable. This distance should not exceed about 4 H_o. If vane length and angle of attack are selected to be L = 2 m and $\alpha = 20^o$, the appropriate graphs are Figures 15g and 16b. By entering these graphs with $F_D = 15.6$ and m = 4 it is seen that a four-vane array will generate a maximum increase in bed level of $(d_o - d_v) = 0.3\ d_o = 0.6$ m. In other words, at the bank the berms will be as high as the vanes. A streamwise spacing between the arrays of $\delta_s = 30\ H_o = 18$ m is appropriate.

If the vane size is increased to $H_o = 1$ m and L = 3 m so that $H_o/d_o = 0.5$ and $H_o/L = 0.3$, and $\alpha = 20^o$ as before, then the graphs would be Figures 15c and 16a. In this case it is sufficient to use three vanes per array, only. The lateral spacing would be $\delta_n = 3\ H_o = 3$ m, and the vane-to-bank distance $\delta_b = 8 - (2)(3) = 2$ m. If the longitudinal spacing is $\delta_s = 30\ H_o = 30$ m, the graph is Figure 16a. It is seen that the increase in bed level at the bank can be expected to be $(d_o - d_v) = 0.48\ d_o = 0.96$ m, i.e., about the height of the vanes. Hence, the larger vanes would create higher berms and fewer vanes would be needed.

To obtain a fully developed berm at the bridge crossing, there must be at least three arrays in the vane system on each side of the channel. The distance from the bridge to the most downstream array should not exceed about 30 H_o.

2. Numerical Example 2

A bridge abutment on the outside bank of a river bend is in danger of being undermined by erosion. At bankfull flow, average width, depth, slope and velocity are b = 50 m, $d_o = 2$ m, S = 0.00075 and $u_o = 1.2$ m/s. Radius of curvature is r = 200 m. The bed material is sand with a median grain diameter of D = 0.6 mm.

The channel's resistance parameter is $m = \kappa u_o/\sqrt{gSd} = (0.4)(1.2)/\sqrt{(9.81)(0.00075)(2)} = 4.0$, which corresponds to a Darcy-Weisbach friction factor of $f = 8\kappa^2/m^2 = 0.08$. The sediment Froude number is $F_D = u_o/\sqrt{gD} = (1.2)/\sqrt{(9.81)(0.6 \times 10^{-3})} = 15.6$, and the channel's width-radius ratio b/r = 0.25. The scour depth along the outer bank at bankfull flow is estimated, by entering the graph in Figure 8 with $F_D(b/r) = (15.6)(0.25) = 3.9$ and m = 4, to be $d = 2.5\ d_o = 5.0$ m.

Erosion at the abutment can be prevented by designing a vane system that at all stages maintains a flow depth along the bank equal to or less than the average flow depth in the channel. This implies that the system at bankfull flow must generate a reduction of near-bank flow depth of $d - d_v = 5.0 - 2.0 = 3.0$ m, or $(d-d_v)/d = 0.60$.

The channel's depth-width ratio is $d_o/b = (2)/(50) = 0.04$. This value is reasonably close to 0.03 for a first estimate, so the appropriate graphs are Figures 11 and 12. It is clear from these graphs that in order to obtain a value of $(d-d_v)/d = 0.6$ with $F_D\ (b/r) = 3.9$ and $m = 4$, there must be at least two vanes in each array.

If vane height, length and angle of attack are selected to be $H_o = 0.6$ m, $L = 2.0$ m and $\alpha = 20^o$, so that $H_o/d_o = 0.3$ and $H_o/L = 0.3$, the appropriate graph is Figure 11g if $\delta_s = 15\ H_o$, and Figure 12b if $\delta_s = 30\ H_o$. By entering Figure 11g with $F_D(b/r) = 3.9$ and $m = 4$ it is seen that a system with two vanes in each array yields $(d-d_v)/d = 0.45$ while a system with three vanes yields $(d-d_v)/d = 0.60$. Consequently, there must be three vanes per array. By entering instead Figure 12b, which applies when $\delta_s = 30H_o$, a system with three vanes per array yields $(d-d_v)/d = 0.48$. The objective will in this case be met with four vanes per array. If the vane size is increased to $H_o = 1.0$ m, $L = 3.0$ m, and $\alpha = 20^o$, so that $H_o/d_o = 0.5$ and $H_o/L = 0.3$, the appropriate graphs are Figures 11c and 12a. In this case it is sufficient to use two vanes per array if $\delta_s = 15\ H_o = 15$ m, and three vanes per array if $\delta_s = 30\ H_o = 30$ m.

In all cases, the lateral spacing of vanes should be $\delta_n = 3\ H_o$ or less. To obtain a fully developed flow situation at the bridge crossing there must be at least three vane arrays upstream from the bridge.

V. TYPICAL VANE LAYOUTS

In many waterways, and very conspicuously around bridges, the bank-erosion problem develops as a result of meandering. As meanders migrate downstream and under a bridge, the flow changes direction relative to the bridge, and the depth profile changes. The most critical situation occurs when the point bar approaches and moves under the bridge. In this case, one abutment and the banks in its vicinity often become subject to undermining and erosion. Figure 33a shows a typical layout of a vane system for protecting abutments on the outside of a river curve against undermining. Included are the typical ranges of the principal dimensions. These ranges also apply to other applications. The layout shown protects the bank by deflecting the main current toward the central portion of the channel.

Figure 33b shows a recommended layout at a bridge waterway with widened cross section at the bridge. A widening of the cross section is often necessary to accommodate overland flows during floods. However, as seen at the Butler County bridge, a widened cross section is prone to shoaling problems. According to the current design guidelines (AASHTO 1987, Richardson et al. 1975), a river channel should normally not be widened unless its slope is increased. An increase in slope would occur if the channel is shortened

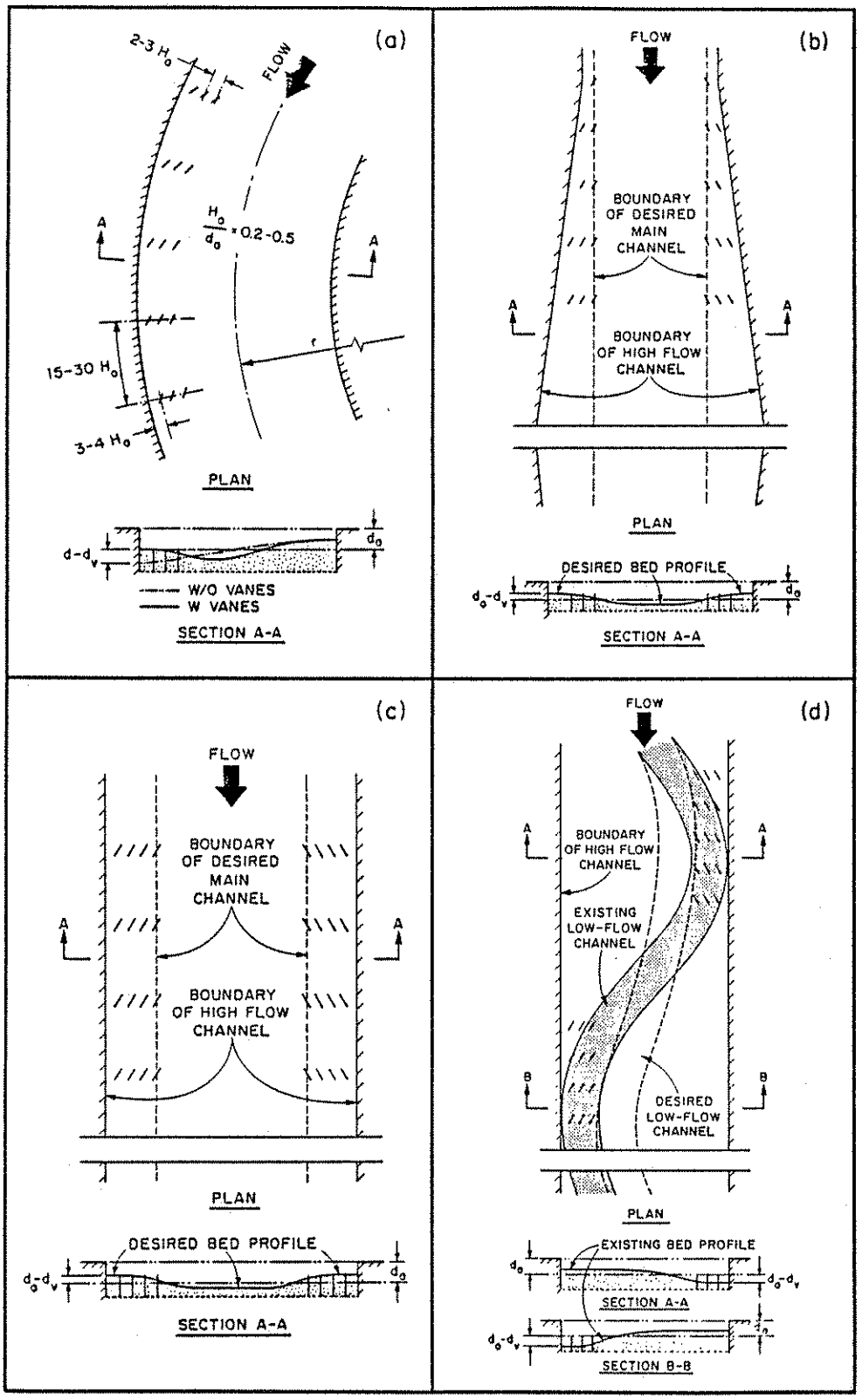

Figure 33. Typical vane layouts for bridge waterways; (a) curved channel; (b) widened channel; (c) straight channel; and (d) straight channel with alternate bars.

by cut-off or realignment. In this case, guidelines indicate that the channel flow can accommodate a widening given by

$$b_2 = \frac{S_2}{S_1} b_1 \tag{37}$$

in which subscript 1 refers to the old channel and subscript 2 to the new channel. The width of the channel at the Butler County bridge was increased from 40 m to 150 m, while the channel slope increased from 0.00049 to 0.00083. Eq. 37 is obtained based on the assumption that the sediment transport capacity q_s is proportional to streampower, i.e.,

$$q_s \sim \tau u \tag{38}$$

By assuming that the sediment transport capacity in the new channel is equal to that in the old channel, i.e., $q_{s1} = q_{s2}$, Eq. 38 yields

$$\tau_1 u_1 = \tau_2 u_2 \tag{39}$$

Eq. 37 is obtained by substitution of $\tau = \rho g S d$ and $u = Q/(bd)$ into Eq. 39 . One of the uncertainties with this guideline is that sediment-transport capacity is not necessarily proportional to streampower or to any power of τu. In fact, most sediment-transport relations reported in the literature are not as simple as that of Eq. 38 suggesting that Eq. 37 may not be a sufficient guideline for widening of a channel. Submerged vanes would reduce the risk of failure associated with this practice. The layout shown would ensure that (1) the main flow passes under the central portion of the bridge, and (2) berms are maintained along the sides of the channel to protect the bridge abutments and the adjacent streambanks. If the flow approaches the bridge at an angle significantly different from 90°, the vanes would be concentrated on one side of the channel as in the case of the Butler County bridge.

A similar layout would be employed also in channels of constant width to improve flood conveyance capacity, maintain a navigation channel, or to locally reduce the amplitude of alternate bars as they pass a bridge or other vulnerable structure or property (Figure 33c). In these cases, the outermost vanes also should edge the desired main channel, and vane height would be selected such that the berms are submerged only during certain flow events. In the alternate bar case, the vane installation may be a two-phase project. In the first phase vanes would be installed in the low-flow channel immediately upstream from the

meander apex, as shown in Figure 33d. These vanes would move the low-flow channel away from the eroding banks and reduce the impact at high flows. As the meanders or bars move downstream the low flow channel, and the high-velocity thread, will be moved to the other side (to the other abutment). This may happen during one storm, or it may take several years. At this point, the second phase of the project is implemented in which vanes are installed opposite from the old vanes in what is now the low flow channel. In many cases, the second phase would consist of completing the layout so that a continuous berm is established along the banks upstream from the critical site (Figure 33c).

VI. VANE MATERIAL

So far, the prototype vane material has varied from project to project. In the Butler County installation, the vanes are constructed from sheet piling (Figure 27). The vanes in the East Nishnabotna River consist of planks supported by H-piles (Figure 34) (Odgaard and Mosconi 1987). In the Japanese project, the vanes are constructed from round wood poles (Figure 35) (Fukuoka 1989, Fukuoka and Watanabe 1989). In these three cases, the vanes are essentially "flat-plate" designs. Such a design is effective as long as vane thickness is small compared with vane length and height. Because of the angle of attack the flow separates at the leading edge of the "plates", and local scour occurs. The Japanese vanes are provided with a relatively large diameter circular column at the leading edge of the vanes. According to Fukuoka and Watanabe (1989), this column reduces local scour and results in somewhat higher efficiency as measured by the amount of sand accumulated per vane. This is probably because the rounded nose reduces the size of the separated zone. The leading edge on the East Nishnabotna vanes is a 20 cm wide flange of the H-piles supporting the vanes. This flange produces considerable separation and local scour and obviously inhibits the generation of circulation.

The vanes in the recent installations in the Wapsipinicon and Cedar Rivers in Iowa are made of reinforced concrete (Figures 36 and 37). Each vane is 0.9 m high, 3 m long and 20 cm thick. It is supported by only one pile. The top portion of the pile is embedded in the vane so that no part of the pile is exposed to the flow. The vane is shaped as a double-curved foil with a twisted rear edge and a rounded nose. Its shape is modeled after the model vanes in the curved laboratory flume. The rounded nose is designed to reduce separation and minimize impact forces due to ice and debris at low flow. The twisted shape occurs as a result of a downward increase in the camber of the vane. This increase in camber is designed so that a certain (elliptic) circulation distribution is maintained along the height of the vane. As the camber increases toward the bed, the effective angle of attack increases. This increase compensates for the decrease in flow velocity near the bed due to

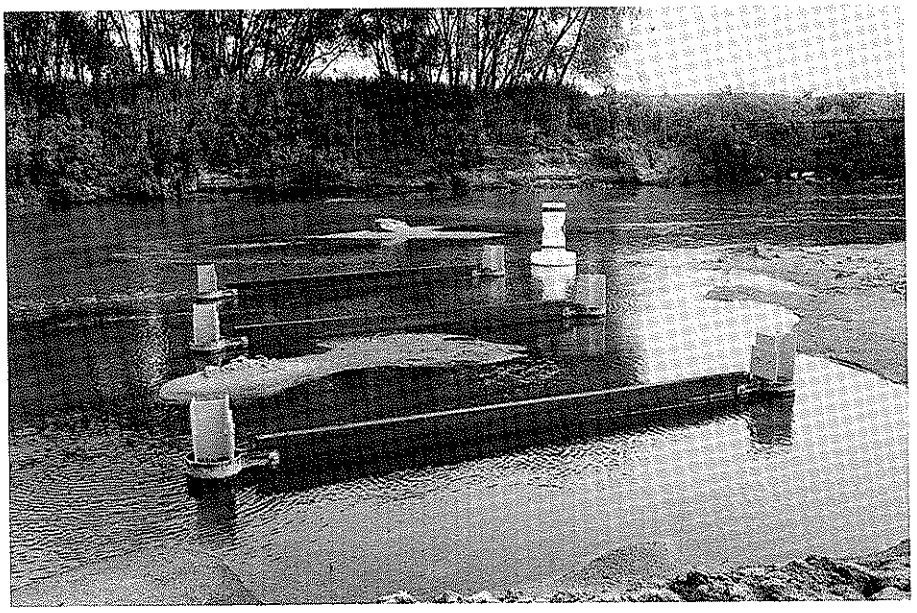

Figure 34. Three-vane array in the East Nishnabotna River installation.

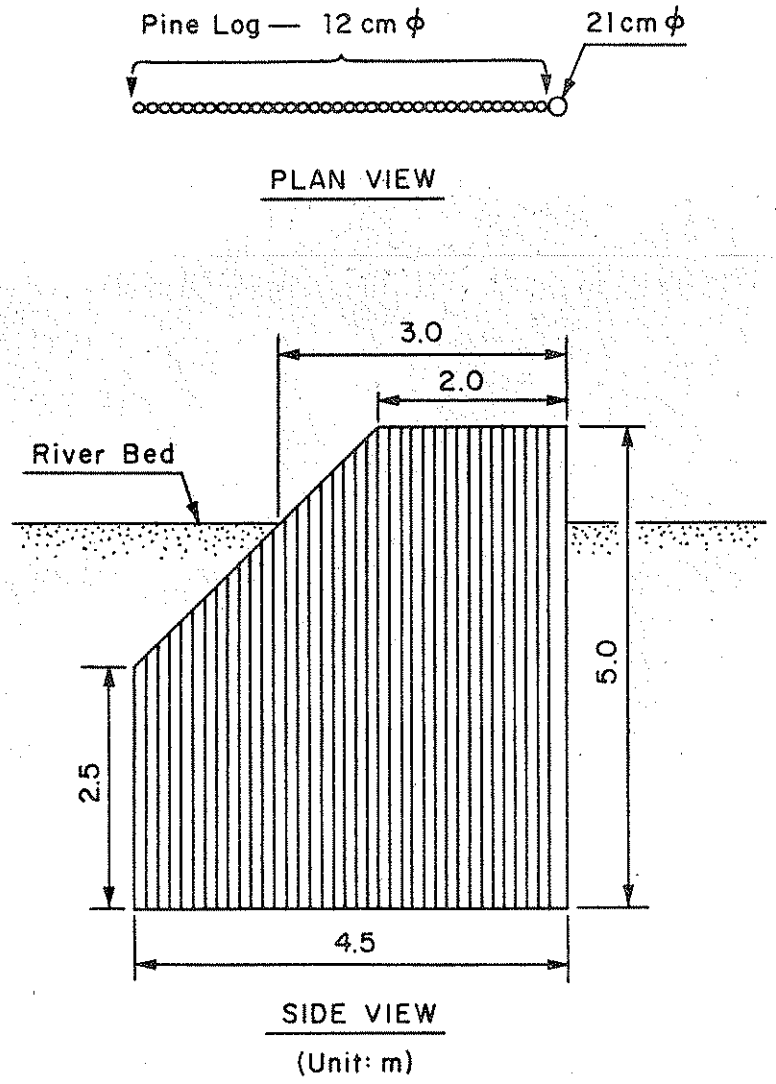

Figure 35. Vane design used in Kuro River, Japan (Fukuoka and Watanabe 1989).

Figure 36. Pile driving for the Wapsipinicon River vane installation. (Courtesy of River Engineering International, Inc., Iowa City, Iowa.)

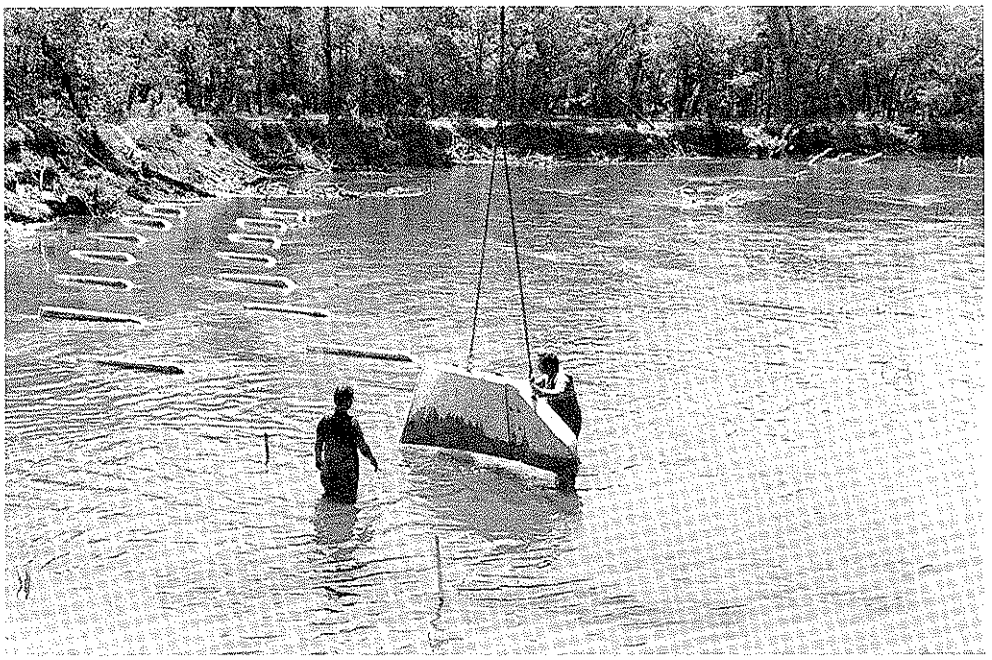

Figure 37. Vane installation in the Wapsipinicon River, Iowa. (Courtesy of River Engineering International, Inc., Iowa City, Iowa.)

bed friction, and the resulting circulation distribution is nearly the same as that associated with a thin, flat plate in a uniform velocity field (Odgaard and Spoljaric 1989). Thus, the shape of the vane produces a nearly ideal circulation distribution despite that the vane is in a boundary layer. This, and its sturdiness, are the main advantages of the twisted design.

It is likely that other materials and designs can also be used. As was mentioned in an earlier paper on this subject (Odgaard and Kennedy 1983), a less sophisticated design consists of rows of dumped rock with steep side slopes. Such "vanes" would achieve much the same result, although more and longer "vanes" of this type likely would be required because of the smaller transverse force per unit area which would be exerted on them. This solution could be attractive, either in itself or in combination with shaped or plane vanes, in deep water where pile driving is difficult. The design guidelines developed herein do not apply to rock vanes.

VII. CONCLUSIONS AND RECOMMENDATIONS

The study has shown that the submerged vanes technique has merits as a general sediment control technique for bridge waterways and rivers in general. By generating secondary circulation in the flow, the vanes alter the distribution of bed shear stresses across the river channel and cause a redistribution of flow velocity and depth. The theory developed in this study relates this redistribution to the parameters of the vane system. Both laboratory and field experience show that this relationship, and hence the design procedure established, are valid. Because of separation on the low pressure side of the vanes, the relative magnitudes of the induced changes in streamwise and transverse bed shear stress components may not be exactly as calculated. However, the tests clearly suggest that the total stress field is well predicted.

It is evident that vanes can produce significant changes in the distributions of velocity and depth. By introducing relatively small changes in the bed shear stresses, arrays of vanes can generate local changes in the bed elevation of the order of the vane height. The major controlling parameters are relative vane height, vane aspect ratio and angle, vane density (number of vanes per unit area), channel resistance and sediment Froude number. An increase of any of these parameters causes the induced changes in bed elevation to increase.

In most applications, the vane height will be between 30 and 50% of bankfull-flow depth and vane length will be two to three times vane height. The vanes will be placed in arrays along the bank of the river. Each array will contain two or more vanes. The vanes in an array will be spaced laterally a distance of two to three times vane height. The

streamwise spacing between the arrays will be 15 to 30 times vane height. The vane-to-bank distance should not exceed four times the vane height. The first (most upstream) array in the vane system must be located a distance of at least three array spacings upstream from the bridge, and there must be at least three arrays in the system for it to be effective at and downstream from the third array.

One of the still uncertain design variables is the longitudinal distance between the vane arrays. In the laboratory tests, this spacing was 12 - 15 times vane height, and the results were good. The theory, however, and the data from the Butler County installation suggest that an array spacing of 30 times vane height is nearly equally effective. Obviously, this design parameter should be further tested.

REFERENCES

AASHTO (1987). "Hydraulic analyses for the location and design of bridges," Highway Drainage Guidelines, American Association of State Highway and Transportation Officials, Inc., Washington, D.C., Vol. VII, p. 185.

Ashida, K., and Michiue, M. (1972). "Study on hydraulic resistance and bedload transport rate in alluvial streams," Trans., Japan Soc. Civ. Engrs., 206, 59-69.

Falcon, M.A. (1979). "Analysis of flow in alluvial channel bends," thesis presented to The University of Iowa, at Iowa City, in partial fulfillment of the requirements for the degree of Doctor of Philosophy.

Fukuoka, S. (1989). "Groins and vanes developed basing upon a new concept of bank protection," Proc., ASCE National Conference on Hydraulic Engineering, New Orleans, LA, 224-229.

Fukuoka, S., and Watanabe, A. (1989). "New bank protection methods against erosion in the river," Proceedings of the Japan-China Joint Seminar on Natural Hazard Mitigation, Kyoto, Japan, July 16-20, pp. 439-448.

Ikeda, S., and Nishimura, T. (1985). "Bed topography in bends of sand-silt rivers," J. Hydr. Engrg., ASCE, 111(11), 1397-1411.

Kikkawa, H., Ikeda, S., and Kitagawa, A. (1976). "Flow and bed topography in curved channels," J. Hydr. Div., ASCE, 102(9), 1317-1342.

Kunzig, R. (1989). "Wandering river," Discover, 10(11), 69-71.

Milne-Thomson, L.M. (1966). Theoretical aerodynamics. Dover Publications, Inc., New York.

Odgaard, A.J. (1986). "Meander flow model. I: Development," J. Hydr. Engrg., ASCE, 112(12), 1117-1136.

Odgaard, A.J. (1989a). "River-meander model. I. Development," J. Hydr. Engrg., 115(11), 1433-1450.

Odgaard, A.J. (1989b). "River-meander model. II: Applications," J. Hydr. Engrg., ASCE, 115(11), 1451-1464.

Odgaard, A.J. and Spoljaric, A. (1986). "Sediment control by submerged vanes," J. Hydr. Engrg., ASCE, 112(12), 1164-1181.

Odgaard, A.J., and DeWitt, R.J. (1989). "Sediment control by submerged vanes," Proc. 20th Annual Conference of the International Erosion Control Association, Vancouver, British Columbia, Canada, Feb. 16-17.

Odgaard, A.J., and Kennedy, J.F. (1983). "River-bend bank protection by submerged vanes," Journal of Hydraulic Engineering, ASCE, 109(8), 1161-1173.

Odgaard, A.J., and Lee, H.Y.E. (1984). "Submerged vanes for flow control and bank protection in streams," IIHR Report No. 279, Iowa Inst. of Hydr. Res., The University of Iowa, Iowa City, IA.

Odgaard, A.J., and Mosconi, C.E. (1987). "Streambank protection by submerged vanes," J. Hydr. Engrg., ASCE, 113(4), 520-536.

Odgaard, A.J. and Bergs, M.A. (1988). "Flow processes in a curved alluvial channel," Water Resources Research, 24(1), 45-56.

Odgaard, A.J., and Spoljaric, A. (1989). "Sediment control by submerged vanes. Design basis," River Meandering, S. Ikeda and G. Parker, eds., American Geophysical Union Water Resources Monograph No. 12, 127-151.

Odgaard, A.J., and Wang, Y. (1990). "Sediment management with submerged vanes. I: Theory," J. Hydr. Engrg., ASCE,

Odgaard, A.J., and Wang, Y. (1990). "Sediment management with submerged vanes. II: Applications," J. Hydr. Engrg., ASCE,

Richardson, E. et al. (1975), "Highways in the river environment, hydraulics and environmental design considerations, training, and design manual," Federal Highway Administration, Washington, D.C., Chapter VI.

Rozovskii, I.L. (1957). Flow of water in bends of open channels. Academy of Sciences of the Ukrainian SSR, Kiev, USSR (in Russian) (English translation, Israel Program for Scientific Translation, Jerusalem, Israel, 1961).

Sabersky, R.H., and Acosta, A.J. (1964). Fluid flow. MacMillan Publishing Co., Inc., New York.

Simons, D.B., and Sentürk, F. (1977). Sediment transport technology, Water Resources Publications, Fort Collins, Colorado.

Wang, Y. (1989). "Bank protection with submerged vanes," Proc., XXIII Congress of IAHR, Int. Assoc. for Hydr. Res., Vol. S, 17-23.

Wang, Y. (1990). "Sediment control with submerged vanes," thesis presented to The University of Iowa, at Iowa City, Iowa, in partial fulfillment of the requirements for the degree of Doctor of Philosophy.

Zimmermann, C., and Kennedy, J.F. (1978). "Transverse bed slopes in curved alluvial streams," J. Hydr. Div., ASCE, 104(1), 33-48.